Published for SISSA by Springer

Received: February 20, 2017
Accepted: May 10, 2017
Published: May 22, 2017

Renormalisation-group improved analysis of $\mu \to e$ processes in a systematic effective-field-theory approach

A. Crivellin,[a] **S. Davidson,**[b,c] **G.M. Pruna**[a] **and A. Signer**[a,d]

[a] *Paul Scherrer Institut, CH-5232 Villigen PSI, Switzerland*
[b] *IPNL, CNRS/IN2P3, 4 rue E. Fermi, 69622 Villeurbanne cedex, France*
[c] *Université de Lyon, F-69622 Lyon, France*
[d] *Physik-Institut, Universität Zürich, Winterthurerstrasse 190, CH-8057 Zürich, Switzerland*

E-mail: Andreas.Crivellin@cern.ch, S.Davidson@ipnl.in2p3.fr, Giovanni-Marco.Pruna@psi.ch, Adrian.Signer@psi.ch

Abstract: In this article, a complete analysis of the three muonic lepton-flavour violating processes $\mu \to e\gamma$, $\mu \to 3e$ and coherent nuclear $\mu \to e$ conversion is performed in the framework of an effective theory with dimension six operators defined below the electroweak symmetry breaking scale m_W. The renormalisation-group evolution of the Wilson coefficients between m_W and the experimental scale is fully taken into account at the leading order in QCD and QED, and explicit analytic and numerical evolution matrices are given. As a result, muonic decay and conversion rates are interpreted as functions of the Wilson coefficients at any scale up to m_W. Taking the experimental limits on these processes as input, the phenomenology of the mixing effects is investigated. It is found that a considerable set of Wilson coefficients unbounded in the simplistic tree-level approach are instead severely constrained. In addition, correlations among operators are studied both in the light of current data and future experimental prospects.

Keywords: Beyond Standard Model, Effective Field Theories, Renormalization Group

ArXiv ePrint: 1702.03020

Open Access, © The Authors.
Article funded by SCOAP[3].

doi:10.1007/JHEP05(2017)117

JHEP05(2017)117

Contents

1 Introduction **1**

2 Low-energy Lagrangian **2**

3 LFV muon decays **4**

3.1 $\mu \to e\gamma$ 4

3.2 $\mu \to eee$ 4

3.3 $\mu \to e$ conversion in nuclei 5

4 Renormalisation-group evolution **6**

5 Phenomenological analysis **11**

6 Conclusions and outlook **19**

A Anomalous dimensions **21**

1 Introduction

Processes involving charged lepton flavour violation (LFV) are very promising places to search for physics beyond the Standard Model (BSM). In the SM with massless neutrinos these processes are forbidden, and even including neutrino masses and mixing these processes are suppressed by ratios m_ν^4/m_W^4. Thus, they are by far too small to be measured in any foreseeable experiment. Therefore, any observation of charged LFV would directly prove the existence of BSM physics. In fact, in many BSM scenarios, such processes can have sizeable decay rates which are naturally in the reach of forthcoming experiments.

Among the charged LFV processes, the category of muonic transitions is particularly interesting, providing three processes with complementary sensitivities to new physics (NP) and stringently constrained by experiment: the current limits from the MEG [1, 2] and SINDRUM [3, 4] collaborations are

$$\mathrm{Br}\left(\mu^+ \to e^+\gamma\right) \leq 4.2 \times 10^{-13}\,, \tag{1.1}$$

$$\mathrm{Br}\left(\mu^+ \to e^+e^-e^+\right) \leq 1.0 \times 10^{-12}\,, \tag{1.2}$$

$$\mathrm{Br}^{\mathrm{Au}}_{\mu\to e} \equiv \frac{\Gamma(\mu^- \mathrm{Au} \to e^- \mathrm{Au})}{\Gamma^{\mathrm{capt}}_{\mathrm{Au}}} \leq 7 \times 10^{-13}\,. \tag{1.3}$$

The future experimental prospects for $\mu \to e$ transitions are also promising. With the upgrade to MEG II [5], the sensitivity of $\mathrm{Br}(\mu \to e\gamma)$ will reach $\sim 5 \times 10^{-14}$. Furthermore, Mu3e will improve the sensitivity on $\mu \to 3e$ by up to 4 orders of magnitude [6]. Concerning $\mu \to e$ conversion in nuclei, the DeeMe experiment aims at an accuracy of 10^{-14} [7], while Mu2e at FNAL and COMET at J-PARC [8–10] aim to improve the sensitivity to the conversion rate by four orders of magnitude compared to SINDRUM II. Moreover, the PRISM/PRIME project [11] aims to reach the remarkable limit of $\mathrm{Br}(\mu \to e) \lesssim 10^{-18}$.

JHEP05(2017)117

LFV processes have been studied in detail in many specific extensions of the SM (for a recent review see for example [12] and references therein). However, in this article an effective-field-theory description of NP interactions is adopted. In this context, Kuno and Okada [13] reviewed $\mu \to e$ flavour-changing processes and experiments, and the operator basis required to parameterise them.

Constraints on Wilson coefficients, usually at the scale of the experiments, have been compiled for LFV 2-lepton-2-quark operators [14, 15] with a tau-lepton [16–18], and 4-lepton operators [19]. In the quark flavour sector, a long-time effort allowed to establish the QCD running of Wilson coefficients (see [20] and references therein).

However, given that the electromagnetic coupling is much smaller than the strong one, $\alpha_e \ll \alpha_s$, QED running is often neglected for the leptons. Czarnecki and Jankowski [21] proved that the self-renormalisation of the $\mu \to e\gamma$ dipole reduces the coefficient at low energy. Also in the case of $(g-2)_\mu$ (lepton-flavour conserving effective interactions), the QED running and mixing among a basis of SM-induced operators has been included [22]. More recently, the one-loop running of an SU(2)-invariant operator basis [23, 24] was presented in [25, 26] and loop effects in the SU(2)-invariant theory were calculated [27, 28].[1] The results of [25, 26, 28] were used in [33], to translate the current $\mu \to e\gamma$ bound from the experimental scale to the new-physics scale, using QED×QCD invariant operators below m_W, and the SU(2)-invariant operators above.[2]

The purpose of this article is to give the renormalisation-group evolution (RGE) between the electroweak-symmetry-breaking (EWSB) scale and the scale at which the experiments are performed. We consider the Wilson coefficients that are relevant for $\mu \to e\gamma$, $\mu \to 3e$ and coherent $\mu \to e$ conversion and include the lowest non-vanishing order in QED and QCD ($\equiv$ leading order). Our analysis extends [33] by including the one-loop RGE of vector operators, and the two-loop mixing of vectors to the dipoles, as well as the inclusion of $\mu \to e$ conversion and $\mu \to 3e$ in the phenomenological analysis. In addition, we include the dimension-seven lepton-gluon operator that is relevant in $\mu \to e$ conversion [35].

The outline of the paper is as follows: section 2 introduces the QCD×QED invariant operators of our effective Lagrangian. The essential formulas for the transition rates of our three processes in terms of the Wilson coefficients of the operators are recalled in section 3. Then, the RGE of these Wilson coefficients is discussed in section 4 with the analytic formulas collected in appendix A. These results are combined in section 5 to obtain limits on various Wilson coefficients and discuss the complementarity of the three processes.

2 Low-energy Lagrangian

Following the Appelquist-Carazzone theorem [36], we consider an effective Lagrangian that is valid below some scale Λ with $m_W \geq \Lambda \gg m_b$. Therefore, it consists of all operators that are invariant under $\mathrm{U}(1)_{\mathrm{QED}} \times \mathrm{SU}(3)_{\mathrm{QCD}}$ and contain the fermion fields $f \in \{u, d, c, s, b, e, \mu, \tau\}$, as well as the QED and QCD gauge fields. In addition to the

[1] For an analogous analysis in the quark sector see for example [29–32].

[2] Restricting to the SU(2)-invariant operators below m_W fails to consider relevant contributions, as shown in [33, 34].

JHEP05(2017)117

dimension-four QED and QCD Lagrangians, it contains higher-dimensional operators multiplied by dimensionless Wilson coefficients C. Having $\mu \to e$ transitions in mind, we restrict ourselves to operators that induce such transitions and are flavour diagonal with respect to the other fields. Concretely, our Lagrangian reads

$$\begin{aligned}\mathcal{L}_{\text{eff}} &= \mathcal{L}_{\text{QED}} + \mathcal{L}_{\text{QCD}} \\ &+ \frac{1}{\Lambda^2}\Bigg\{ C_L^D O_L^D + \sum_{f=q,\ell} \left(C_{ff}^{V\,LL} O_{ff}^{V\,LL} + C_{ff}^{V\,LR} O_{ff}^{V\,LR} + C_{ff}^{S\,LL} O_{ff}^{S\,LL} \right) \\ &\quad + \sum_{h=q,\tau} \left(C_{hh}^{T\,LL} O_{hh}^{T\,LL} + C_{hh}^{S\,LR} O_{hh}^{S\,LR} \right) + C_{gg}^L O_{gg}^L + L \leftrightarrow R \Bigg\} + \text{h.c.},\end{aligned} \tag{2.1}$$

with the explicit form of the operators given by

$$O_L^D = e\, m_\mu \left(\bar{e}\sigma^{\mu\nu} P_L \mu\right) F_{\mu\nu}, \tag{2.2}$$

$$O_{ff}^{V\,LL} = \left(\bar{e}\gamma^\mu P_L \mu\right)\left(\bar{f}\gamma_\mu P_L f\right), \tag{2.3}$$

$$O_{ff}^{V\,LR} = \left(\bar{e}\gamma^\mu P_L \mu\right)\left(\bar{f}\gamma_\mu P_R f\right), \tag{2.4}$$

$$O_{ff}^{S\,LL} = \left(\bar{e} P_L \mu\right)\left(\bar{f} P_L f\right), \tag{2.5}$$

$$O_{hh}^{S\,LR} = \left(\bar{e} P_L \mu\right)\left(\bar{h} P_R h\right), \tag{2.6}$$

$$O_{hh}^{T\,LL} = \left(\bar{e}\sigma_{\mu\nu} P_L \mu\right)\left(\bar{h}\sigma^{\mu\nu} P_L h\right), \tag{2.7}$$

$$O_{gg}^L = \alpha_s\, m_\mu G_F \left(\bar{e} P_L \mu\right) G_{\mu\nu}^a G_a^{\mu\nu}, \tag{2.8}$$

where $P_{L/R} = \left(\mathbb{I} \mp \gamma^5\right)/2$. The field-strength tensors for photons and gluons are denoted by $F^{\mu\nu}$ and $G_a^{\mu\nu}$, respectively. Regarding the matter fields, f represents any fermion below the decoupling scale m_W, and $h \in \{u, d, c, s, b, \tau\}$ is restricted to be either a quark (hadron) or the τ (heavy lepton). Note that for $f \in \{e, \mu\}$, the tensor $O_{ff}^{T\,LL}$, $O_{ff}^{T\,RR}$ and scalar $O_{ff}^{S\,LR}$, $O_{ff}^{S\,RL}$ operators can be reduced by Fierz transformations to other operators already present in $\mathcal{L}_{\text{eff}}$. Therefore, this Lagrangian does not contain redundant operators and constitutes a minimal basis.

Concerning the dipole operators O_L^D and O_R^D, the fields only add up to dimension 5. Thus, they cannot mix into the four-fermion operators (due to renormalisability arguments), although the latter can mix into the dipole operators. Since the dipole operators flip chirality we have defined them by including a factor of m_μ, enhancing their dimensionality up to 6. Also, the prefactor e included in O_L^D and O_R^D is introduced for convenience (when considering the RGE).

Following [35], the only dimension 7 operators that we include in eq. (2.8) are O_{gg}^L and O_{gg}^R. These operators are phenomenologically relevant because, as shown in [37], they encode the effects of scalar operators with heavy quarks (i.e. c, b) below the heavy-quark mass scale m_Q, after the matching has been performed. In practical terms, these operators are suppressed by $1/(\Lambda^2 m_Q)$ rather than $1/(\Lambda^3)$. The normalisation of these operators has been chosen such that their Wilson coefficients do not run under QCD at one loop and the factor G_F is included to resize the dimensionality down to 6.

In the scenario where BSM physics is realised at a scale $\Lambda < m_W$, this NP directly gives rise to the higher-dimensional operators in $\mathcal{L}_{\text{eff}}$. If BSM physics is beyond the EWSB scale,

JHEP05(2017)117

as it is usually assumed, SU(2) invariant higher-dimensional operators are first generated in the Standard Model Effective Field Theory (SMEFT). Then, the higher-dimensional operators in $\mathcal{L}_{\text{eff}}$ stem from the matching of the SMEFT to our theory, as performed at tree level in [33]. It is clear that $\mathcal{L}_{\text{eff}}$ cannot be a valid description of nature above the EWSB scale, as it does not respect the SU(2) symmetry.

However, we stress the fact that if NP is realised not too far above the EWSB scale, then a reduced hierarchy between the NP and EWSB scales would not allow for potential large logarithms from the SMEFT RGE, while the hierarchy between the EWSB scale (our matching scale) and the muon/nuclear scale is always sufficiently large to give rise to important effects.

3 LFV muon decays

In this section, the expressions for the processes $\mu^+ \to e^+\gamma$, $\mu^+ \to e^+e^-e^+$, and coherent muon-to-electron conversion in muonic atoms $\mu^- N \to e^- N$ in terms of the coefficients C_i of the Lagrangian eq. (2.1) will be presented. We restrict ourselves to the tree-level expressions. Loop effects are only included through the RGE of the Wilson coefficients. Thus, for the expressions that follow the Wilson coefficients are understood to be evaluated at the scale of the process.

3.1 $\mu \to e\gamma$

Currently, $\mu^+ \to e^+\gamma$ is the LFV muonic process with the most stringent experimental bound [1]. At the tree level, the Lagrangian in eq. (2.1) results in the branching ratio

$$\text{Br}\left(\mu \to e\gamma\right) = \frac{\alpha_e m_\mu^5}{\Lambda^4 \Gamma_\mu} \left(\left|C_L^D\right|^2 + \left|C_R^D\right|^2 \right) , \tag{3.1}$$

where Γ_μ is the width of the muon. The scale of the process is $\mu = m_\mu$. Operators other than the dipole will enter this process only through the RGE.

3.2 $\mu \to eee$

The bounds on $\mu \to 3e$ are already very precise, but Mu3e will significantly improve them in the coming years [6]. The branching ratio expressed in terms of Wilson coefficients $C_i(m_\mu)$ reads

$$\begin{aligned} \text{Br}(\mu \to 3e) = {} & \frac{\alpha_e^2 m_\mu^5}{12\pi\Lambda^4\Gamma_\mu} \left(\left|C_L^D\right|^2 + \left|C_R^D\right|^2 \right) \left(8 \log\left[\frac{m_\mu}{m_e}\right] - 11 \right) + X_\gamma \\ & + \frac{m_\mu^5}{3(16\pi)^3\Lambda^4\Gamma_\mu} \Big(\left|C_{ee}^{S\,LL}\right|^2 + 16 \left|C_{ee}^{V\,LL}\right|^2 + 8 \left|C_{ee}^{V\,LR}\right|^2 \\ & \qquad + \left|C_{ee}^{S\,RR}\right|^2 + 16 \left|C_{ee}^{V\,RR}\right|^2 + 8 \left|C_{ee}^{V\,RL}\right|^2 \Big) , \end{aligned} \tag{3.2}$$

where the interference term with the dipole operator is given by

$$X_\gamma = -\frac{\alpha_e m_\mu^5}{3(4\pi)^2\Lambda^4\Gamma_\mu} \Big(\text{Re}\Big[C_L^D \left(C_{ee}^{V\,RL} + 2C_{ee}^{V\,RR} \right)^* \Big] + \text{Re}\Big[C_R^D \left(2C_{ee}^{V\,LL} + C_{ee}^{V\,LR} \right)^* \Big] \Big) . \tag{3.3}$$

JHEP05(2017)117

Notice that interference between the four-lepton operators can be neglected because it is suppressed by powers of m_e. So in contrast to $\mu \to e\gamma$ and coherent $\mu \to e$ conversion, which only impose two constraints, the upper bound on $\mathrm{Br}(\mu \to 3e)$ sets independent constraints on several four-lepton operators. Through the RGEs, this process is also sensitive to operators involving quarks or other leptons.

3.3 $\mu \to e$ conversion in nuclei

The coherent LFV muonic transition in nuclei is produced by the dipole, the vector, and the scalar operators already at the tree level [38]. Once relativistic and finite nuclear size effects are taken into account for heavy nuclei [38–40], the transition amplitudes for the three classes of operators exhibit different sensitivities to the atomic number Z. Hence, in principle different target atoms provide different limits on the coefficients of the involved class of operators [35]. Whether it is feasible to perform measurements for many different elements remains to be seen. The SINDRUM collaboration has presented limits for gold, titanium and lead [4, 41, 42], but the upcoming experiments mostly concentrate on aluminium.

For this process, the Lagrangian $\mathcal{L}_{\text{eff}}$ as given in eq. (2.1) is not directly suitable. Instead, a Lagrangian at the nucleon level containing proton and neutron fields is required. This Lagrangian is obtained in two steps. First, heavy quarks are integrated out. This results in a redefinition of the Wilson coefficient of the gluonic operator [37]

$$C_{gg}^{L} \to \tilde{C}_{gg}^{L} = C_{gg}^{L} - \frac{1}{12\pi} \sum_{q=c,b} \frac{C_{qq}^{S\,LL} + C_{qq}^{S\,LR}}{G_F\, m_\mu m_q} \tag{3.4}$$

with an analogous equation for C_{gg}^{R}. Second, the resulting Lagrangian is matched at a scale of $\mu_n = 1\,\text{GeV}$ to an effective Lagrangian at the nucleon level. Following [35] the transition rate $\Gamma_{\mu\to e}^{N} = \Gamma(\mu^- N \to e^- N)$ can then be written as

$$\Gamma_{\mu\to e}^{N} = \frac{m_\mu^5}{4\Lambda^4} \left| e\, C_L^D\, D_N + 4 \left(G_F m_\mu m_p \tilde{C}_{(p)}^{SL} S_N^{(p)} + \tilde{C}_{(p)}^{VR}\, V_N^{(p)} + p \to n \right) \right|^2 + L \leftrightarrow R, \tag{3.5}$$

where p and n denote the proton and the neutron, respectively. The effective couplings in eq. (3.5) can be expressed in terms of our Wilson coefficients as

$$\tilde{C}_{(p/n)}^{VR} = \sum_{q=u,d,s} \left(C_{qq}^{V\,RL} + C_{qq}^{V\,RR} \right)\, f_{Vp/n}^{(q)}\,, \tag{3.6}$$

$$\tilde{C}_{(p/n)}^{SL} = \sum_{q=u,d,s} \frac{\left(C_{qq}^{S\,LL} + C_{qq}^{S\,LR} \right)}{m_\mu m_q G_F}\, f_{Sp/n}^{(q)} + \tilde{C}_{gg}^{L}\, f_{Gp/n} \tag{3.7}$$

with analogous relations for $L \leftrightarrow R$. The Wilson coefficients in eqs. (3.6) and (3.7) are to be evaluated at the scale μ_n.

The nucleon form factors for vector operators are known from the vector-current conservation, i.e. $f_{Vp}^{(u)} = 2$, $f_{Vn}^{(u)} = 1$, $f_{Vp}^{(d)} = 1$, $f_{Vn}^{(d)} = 2$, $f_{Vp}^{(s)} = 0$, $f_{Vn}^{(s)} = 0$. Hence, the sum in eq. (3.6) is in fact only over $q = u, d$. The calculation of the scalar form factors is more involved. Following [43], the values of the up- and down-quark scalar couplings $f_{Sp/n}^{(u/d)}$ from [44] (based on the two-flavour chiral perturbation theory framework of [45])

JHEP05(2017)117

are used. The values of the s-quark scalar couplings $f^{(s)}_{Sp/n}$ are borrowed from a lattice calculation [46].[3] In summary, we use

$$\begin{aligned} f^{(u)}_{Sp} &= (20.8 \pm 1.5) \times 10^{-3}, & f^{(u)}_{Sn} &= (18.9 \pm 1.4) \times 10^{-3}, \\ f^{(d)}_{Sp} &= (41.1 \pm 2.8) \times 10^{-3}, & f^{(d)}_{Sn} &= (45.1 \pm 2.7) \times 10^{-3}, \\ f^{(s)}_{Sp} &= f^{(s)}_{Sn} = (53 \pm 27) \times 10^{-3}. \end{aligned} \tag{3.8}$$

The form factor for the gluonic operator can be obtained from a sum rule. In our normalisation we get

$$f_{Gp/n} = -\frac{8\pi}{9}\left(1 - \sum_{q=u,d,s} f^{(q)}_{Sp/n}\right). \tag{3.9}$$

The quantities D_N, $S_N^{(p/n)}$, and $V_N^{(p/n)}$ in eq. (3.5) are related to the overlap integrals [40] between the lepton wave functions and the nucleon densities. They depend on the nature of the target N and we use the numerical values [38]

$$\begin{aligned} &D_{\rm Au} = 0.189, \quad S^{(p)}_{\rm Au} = 0.0614, \quad V^{(p)}_{\rm Au} = 0.0974, \quad S^{(n)}_{\rm Au} = 0.0918, \quad V^{(n)}_{\rm Au} = 0.146; \\ &D_{\rm Al} = 0.0362, \quad S^{(p)}_{\rm Al} = 0.0155, \quad V^{(p)}_{\rm Al} = 0.0161, \quad S^{(n)}_{\rm Al} = 0.0167, \quad V^{(n)}_{\rm Al} = 0.0173; \end{aligned} \tag{3.10}$$

for gold and aluminium, respectively. The branching ratio is defined as the transition rate, eq. (3.5), divided by the capture rate. For the latter we use

$$\Gamma^{\rm capt}_{\rm Au} = 8.7 \times 10^{-15}\ {\rm MeV}, \qquad \Gamma^{\rm capt}_{\rm Al} = 4.6 \times 10^{-16}\ {\rm MeV}, \tag{3.11}$$

taken from [49].

4 Renormalisation-group evolution

The operators present in $\mathcal{L}_{\rm eff}$, eq. (2.1), will give rise to $\mu \to e$ transitions. Thus, experimental constraints from these processes can be translated into bounds on the coefficients of various operators. However, in the first instance this procedure results in bounds on $C(m_\mu)$ or $C(\mu_n)$, the Wilson coefficients evaluated at the low scale. In order to gain more insight into possible NP scenarios, it is preferable to extract limits on $C(\Lambda)$, i.e. on the Wilson coefficients at the high scale. If $\Lambda < m_W$, this will be directly at the NP scale. If the BSM scale is higher than the EWSB scale, our theory will have to be matched to the SMEFT and, in a second step, the RGE within the SMEFT [25, 26] will have to be carried out from m_W to the scale, where the BSM theory is to be matched to the SMEFT.

Under the RGE, the various operators in $\mathcal{L}_{\rm eff}$ mix among each other. In our analysis, we take into account at least the one-loop anomalous dimensions for all the operators. Since the dipole operator plays a prominent role in all $\mu \to e$ transitions, we also consider those two-loop effects of direct mixing into C^D_L and C^D_R that are "leading", i.e. those with vanishing one-loop contribution.

[3] See [47, 48] for analogous results obtained from a computation in an effective-field theoretical framework.

JHEP05(2017)117

At one loop, the structure of the anomalous dimension matrix splits into two blocks, the vector operators and all the other operators. The dipole operator Q_L^D receives contributions from itself [21, 28], $Q_{ee}^{S\,LL}$, $Q_{\mu\mu}^{S\,LL}$ and $Q_{hh}^{T\,LL}$ [33, 35], and the scalar and tensor operators also mix among themselves. In addition the dimension 7 gluon operators mixes into the quark scalar operators. On the other side, the vector operators mix among themselves [50], but are not connected to the remaining operators.

Many of the anomalous dimensions we need can be found in the literature. However, we have performed an independent computation of all one-loop anomalous dimensions in our basis. In order to perform such a calculation in an automated way, several openly available tools were used: the described model was implemented in `FeynRules v2.3` [51] to obtain consistent Feynman rules;[4] the FeynArts interface of FeynRules was exploited to produce a model file for the `FeynArts v3.9` [52] and `FormCalc v9.2` [53, 54] packages; the combined packages FeynArts/FormCalc were employed to generate non-integrated amplitudes to be elaborated afterwards with the symbolic manipulation system `Form v4.1` [55].

At two loops, also the vector operators mix into dipole operators. Since this mixing is not induced through one-loop diagrams, then the two-loop contributions $\mathcal{O}(\alpha_e)$ are the leading order effect. In general, the corresponding anomalous dimensions are regularisation-scheme dependent. This issue has received a lot of attention in the context of $b \to s\gamma$ transitions [56, 57]. For a physical quantity, this scheme dependence is cancelled by the corresponding scheme dependence of the one-loop finite contributions. In fact, this contribution is of the same order in the coupling, namely $\mathcal{O}(\alpha_e)$. Here, we present our two-loop anomalous dimensions for vector operators in the 't Hooft-Veltman (HV) scheme, where the finite one-loop contribution vanishes. They have been extracted from [57] and are given in appendix A. This can also be done for those scalar operators ($O_{hh}^{S\,LR}$ and $O_{hh}^{S\,RL}$) that can be interchanged with vector operators by Fierz transformations. We remark that our approach, while phenomenologically useful, it is not completely self-consistent and should not be understood as a replacement of a two-loop precision calculation, but rather as a qualitative indication of a leading order effect.

Assembling the Wilson coefficients in a vector $\vec{C}(\mu)$, the renormalisation-group running can be written in matrix form as

$$\begin{aligned}\mu\frac{\mathrm{d}}{\mathrm{d}\mu}\vec{C}(\mu) &= \frac{1}{4\pi}\,\Gamma^0\vec{C} + \frac{\alpha_s}{4\pi}\,\Gamma^s\vec{C} + \frac{\alpha_e}{4\pi}\,\Gamma^e\vec{C} = \\ &= \frac{8\pi^2}{e^2}\Gamma_{ST}\vec{C} + \frac{36\pi^2}{e^2}\Gamma_V\vec{C} + 96\pi^2\Gamma_{VD}\vec{C}\,,\end{aligned} \tag{4.1}$$

where Γ^i are the transpose of the anomalous dimension matrices. The analytic results for the Γ_{ST} (scalar-tensor mixing) are shown in table 1, and for the Γ_V (vector mixing) and Γ_{VD} (vector into dipole mixing) in the upper squared block and last row of table 2, respectively. The complete expressions, keeping small mass ratios and charge factors are collected in appendix A.

[4]The model file is available upon request.

JHEP05(2017)117

$\frac{8\pi^2}{e^2}\mu\frac{\mathrm{d}}{\mathrm{d}\mu}$	$C^{S\,LL}_{ee/\mu\mu}$	$C^{S\,LL}_{\tau\tau}$	$C^{T\,LL}_{\tau\tau}$	$C^{S\,LL}_{uu/cc}$	$C^{T\,LL}_{uu/cc}$	$C^{S\,LL}_{dd/ss/bb}$	$C^{T\,LL}_{dd/ss/bb}$	$C^{S\,LR}_{\tau\tau}$	$C^{S\,LR}_{uu/cc}$	$C^{S\,LR}_{dd/ss/bb}$	C^{D}_{L}
$C^{S\,LL}_{ee/\mu\mu}$	6	0	0	0	0	0	0	0	0	0	0
$C^{S\,LL}_{\tau\tau}$	0	-6	-48	0	0	0	0	0	0	0	0
$C^{T\,LL}_{\tau\tau}$	0	-1	2	0	0	0	0	0	0	0	0
$C^{S\,LL}_{uu/cc}$	0	0	0	$-\frac{13}{3}-4\frac{g_s^2}{e^2}$	32	0	0	0	0	0	0
$C^{T\,LL}_{uu/cc}$	0	0	0	$\frac{2}{3}$	$\frac{13}{9}+4\frac{g_s^2}{e^2}$	0	0	0	0	0	0
$C^{S\,LL}_{dd/ss/bb}$	0	0	0	0	0	$-\frac{10}{3}-4\frac{g_s^2}{e^2}$	-16	0	0	0	0
$C^{T\,LL}_{dd/ss/bb}$	0	0	0	0	0	$-\frac{1}{3}$	$\frac{10}{9}+\frac{4}{3}\frac{g_s^2}{e^2}$	0	0	0	0
$C^{S\,LR}_{\tau\tau}$	0	0	0	0	0	0	0	-6	0	0	0
$C^{S\,LR}_{uu/cc}$	0	0	0	0	0	0	0	0	$-\frac{13}{3}-4\frac{g_s^2}{e^2}$	0	0
$C^{S\,LR}_{dd/ss/bb}$	0	0	0	0	0	0	0	0	0	$-\frac{10}{3}-4\frac{g_s^2}{e^2}$	0
C^{D}_{L}	$\frac{m_{e/\mu}}{2e^2 m_\mu}$	0	$-\frac{4m_\tau}{e^2 m_\mu}$	0	$\frac{8m_c}{e^2 m_\mu}$	0	$-\frac{4m_b}{e^2 m_\mu}$	0	0	0	-8

Table 1. Entries of the transposed anomalous dimension matrix Γ_{ST} for the scalar-tensor sector.

$\frac{36\pi^2}{e^2}\mu\frac{\mathrm{d}}{\mathrm{d}\mu}$	$C^{V\,RR}_{ee}$	$C^{V\,RR}_{\mu\mu}$	$C^{V\,RR}_{\tau\tau}$	$C^{V\,RL}_{ee}$	$C^{V\,RL}_{\mu\mu}$	$C^{V\,RL}_{\tau\tau}$	$C^{V\,RR}_{dd}$	$C^{V\,RR}_{ss}$	$C^{V\,RR}_{bb}$	$C^{V\,RL}_{dd}$	$C^{V\,RL}_{ss}$	$C^{V\,RL}_{bb}$	$C^{V\,RR}_{uu}$	$C^{V\,RR}_{cc}$	$C^{V\,RL}_{uu}$	$C^{V\,RL}_{cc}$
$C^{V\,RR}_{ee}$	33	6	3	3	3	3	3	3	3	3	3	3	-6	-6	-6	-6
$C^{V\,RR}_{\mu\mu}$	6	33	3	3	3	3	3	3	3	3	3	3	-6	-6	-6	-6
$C^{V\,RR}_{\tau\tau}$	6	6	30	3	3	3	3	3	3	3	3	3	-6	-6	-6	-6
$C^{V\,RL}_{ee}$	6	6	3	-24	3	3	3	3	3	3	3	3	-6	-6	-6	-6
$C^{V\,RL}_{\mu\mu}$	6	6	3	3	-24	3	3	3	3	3	3	3	-6	-6	-6	-6
$C^{V\,RL}_{\tau\tau}$	6	6	3	3	3	-24	3	3	3	3	3	3	-6	-6	-6	-6
$C^{V\,RR}_{dd}$	2	2	1	1	1	1	10	1	1	1	1	1	-2	-2	-2	-2
$C^{V\,RR}_{ss}$	2	2	1	1	1	1	1	10	1	1	1	1	-2	-2	-2	-2
$C^{V\,RR}_{bb}$	2	2	1	1	1	1	1	1	10	1	1	1	-2	-2	-2	-2
$C^{V\,RL}_{dd}$	2	2	1	1	1	1	1	1	1	-8	1	1	-2	-2	-2	-2
$C^{V\,RL}_{ss}$	2	2	1	1	1	1	1	1	1	1	-8	1	-2	-2	-2	-2
$C^{V\,RL}_{bb}$	2	2	1	1	1	1	1	1	1	1	1	-8	-2	-2	-2	-2
$C^{V\,RR}_{uu}$	-4	-4	-2	-2	-2	-2	-2	-2	-2	-2	-2	-2	-14	4	4	4
$C^{V\,RR}_{cc}$	-4	-4	-2	-2	-2	-2	-2	-2	-2	-2	-2	-2	4	-14	4	4
$C^{V\,RL}_{uu}$	-4	-4	-2	-2	-2	-2	-2	-2	-2	-2	-2	-2	4	4	22	4
$C^{V\,RL}_{cc}$	-4	-4	-2	-2	-2	-2	-2	-2	-2	-2	-2	-2	4	4	4	22
$96\pi^2 C^{D}_{L}$	174	174	87	-150	-150	-75	11	11	11	-7	-7	-7	32	32	-40	-40

Table 2. Entries of the transposed anomalous dimension matrices Γ_V (upper squared block) and Γ_{VD} (last row) for the vector operators. The last row determines the two-loop mixing of the vector operators into the dipole operator.

JHEP05(2017)117

In the evolution, the operators involving bottom quarks, taus and charm quarks are integrated down to the various thresholds. Concerning the two-loop running of the dipole operator, we remark that the threshold effects result in vanishing one-loop contributions in the 't Hooft-Veltman (HV) scheme. Operators involving light quarks are not meaningful any longer for scales below $\mu_n = 1\,\text{GeV}$. At about this scale, our theory should be matched to a nuclear effective theory (following the same approach that we adopted for the $\mu \to e$ conversion in section 3.3). Concerning the RGE evolution, we also integrate out the light quark operators at 1 GeV.

In order to illustrate the numerical importance of the various terms, we express the Wilson coefficients at a low scale in terms of the Wilson coefficients at $\mu = m_W$. To this end, we decompose the vector $\vec{C} = (C_L^D, \vec{C}_l^{ST}, \vec{C}_q^{ST}, \vec{C}^V, C_{gg}^L)$, where

$$\begin{aligned}
\vec{C}_l^{ST} &= \big(C_{ee}^{S\,LL}, C_{\mu\mu}^{S\,LL}, C_{\tau\tau}^{S\,LL}, C_{\tau\tau}^{T\,LL}, C_{\tau\tau}^{S\,LR}\big),\\
\vec{C}_q^{ST} &= \big(C_{dd}^{S\,LL}, C_{dd}^{T\,LL}, C_{dd}^{S\,LR}, C_{ss}^{S\,LL}, C_{ss}^{T\,LL}, C_{ss}^{S\,LR}, C_{bb}^{S\,LL}, C_{bb}^{T\,LL}, C_{bb}^{S\,LR},\\
&\qquad C_{uu}^{S\,LL}, C_{uu}^{T\,LL}, C_{uu}^{S\,LR}, C_{cc}^{S\,LL}, C_{cc}^{T\,LL}, C_{cc}^{S\,LR}\big),\\
\vec{C}^V &= \big(C_{ee}^{V\,RR}, C_{ee}^{V\,RL}, C_{\mu\mu}^{V\,RR}, C_{\mu\mu}^{V\,RL}, C_{\tau\tau}^{V\,RR}, C_{\tau\tau}^{V\,RL},\\
&\qquad C_{dd}^{V\,RR}, C_{dd}^{V\,RL}, C_{ss}^{V\,RR}, C_{ss}^{V\,RL}, C_{bb}^{V\,RR}, C_{bb}^{V\,RL}, C_{uu}^{V\,RR}, C_{uu}^{V\,RL}, C_{cc}^{V\,RR}, C_{cc}^{V\,RL}\big)\,,
\end{aligned} \tag{4.2}$$

with an analogous expression for the $L \leftrightarrow R$ interchange. The structure of the solution to the RGE, eq. (4.1), can then be written as

$$\begin{pmatrix} C_L^D(m_\mu) \\ \vec{C}_l^{ST}(m_\mu) \\ \vec{C}_q^{ST}(\mu_n) \\ \vec{C}^V(m_\mu) \\ C_{gg}^L(\mu_n) \end{pmatrix} = \begin{pmatrix} U_{DD} & U_{Dl}^{1\times5} & U_{Dq}^{1\times15} & U_{DV}^{1\times16} & U_{Dg} \\ 0^{5\times1} & U_{ll}^{5\times5} & 0^{5\times15} & 0^{5\times16} & 0^{5\times1} \\ 0^{15\times1} & 0^{15\times5} & U_{qq}^{15\times15} & 0^{15\times16} & U_{qg}^{15\times1} \\ 0^{16\times1} & 0^{16\times5} & 0^{16\times15} & U_{VV}^{16\times16} & 0^{16\times1} \\ 0 & 0^{1\times5} & 0^{1\times15} & 0^{1\times16} & U_{gg} \end{pmatrix} \cdot \begin{pmatrix} C_L^D(m_W) \\ \vec{C}_l^{ST}(m_W) \\ \vec{C}_q^{ST}(m_W) \\ \vec{C}^V(m_W) \\ C_{gg}^L(m_W) \end{pmatrix} \tag{4.3}$$

The choice of the low scale in the various parts of $\vec{C}$ on the l.h.s. of eq. (4.3) and the evolution from μ_n to m_μ deserves some comments.[5]

We start by noting that C_L^D, the first entry of $\vec{C}_l^{ST}$ and the first two entries of $\vec{C}^V$ contribute to either $\mu \to e\gamma$ or $\mu \to 3e$, eqs. (3.1) and (3.2). Hence, they have to be evolved down to the scale $\mu = m_\mu$, relevant for these processes. Since this scale is not in the perturbative domain of QCD this is potentially problematic. Fortunately, none of the corresponding anomalous dimensions receives contributions from Γ^s. This leaves us with contributions from light-quark operators which *per se* are not meaningful at a scale below $\mu_n = 1\,\text{GeV}$. However, the mixing of the corresponding tensor operators into the dipole operator, eq. (A.2), is suppressed by light-quark masses. Furthermore, the mixing

[5]Here we remark that the different running scales are introduced in the present discussion for illustrative purpose only. In the phenomenological analysis of section 5 we have consistently extended the running of all Wilson coefficients to the physical scale of the process, namely m_μ for $\mu \to e\gamma$ and $\mu \to 3e$ and μ_n for $\mu \to e$ in nuclei.

JHEP05(2017)117

of light-quark vector operators into C^V_{ee}, eqs. (A.3) and (A.4), relevant for $\mu \to 3e$ modifies $C^V_{ee}(m_\mu)$ only marginally. This leaves us with the two-loop contributions of the light-quark vector operators to the dipole. While the entries of the corresponding evolution matrix $U^{1\times 16}_{DV}$ does depend on how the evolution from μ_n to m_μ is treated, these effects overall are so small that they do not noticeably affect the limits we will present in section 5. Hence we can safely stop the evolution of the light-quark operators at $\mu_n = 1\,\text{GeV}$, even those that are part of $\vec{C}^V(m_\mu)$.

Regarding the remaining two coefficients on the l.h.s. of eq. (4.3) we remark that only $\vec{C}^{ST}_q$ receives contributions involving α_s. Furthermore, $\vec{C}^{ST}_q$ contributes to $\mu \to e$ conversion, eq. (3.7). As discussed in section 3, the relevant scale for this process is μ_n. A similar remark applies to C^L_{gg} even though this coefficient does not run at all. Thus, the evolution of $\vec{C}^{ST}_q$ below the scale $\mu_n = 1\,\text{GeV}$ is neither possible, nor required.

All entries of $U^{1\times 16}_{DV}$ are two-loop contributions. The last entry of $U^{1\times 5}_{Dl}$ and several entries of $U^{1\times 15}_{Dq}$ also receive leading two-loop contributions. The other contributions to the evolution matrices are one loop.

For the presentation of the evolution matrices in the remainder of this section we will set the light-quark masses to zero and stop the evolution of the light-quark operators at μ_n. While this will affect some of the entries of eq. (4.3), these choices have no notable influence on the limits presented in section 5. With these conventions, the numerical values for the entries of eq. (4.3) are the following:

$$\begin{aligned}
U_{DD}(m_\mu, m_W) &= 0.94 \\
U^{1\times 5}_{Dl}(m_\mu, m_W) &= (-0.0002,\ -0.04,\ 0.008,\ 3.2,\ -0.001) \\
U^{1\times 15}_{Dq}(m_\mu, m_W) &= (0,\ 0,\ 0,\ 0,\ 0,\ 0,\ 0.003,\ 4.6,\ -0.0006,\ 0,\ 0,\ 0,\ 0.007,\ -2.7,\ -0.0008) \\
U^{1\times 16}_{DV}(m_\mu, m_W) &= 10^{-4}\ (-3.1,\ 1.4,\ -3.1,\ 3.5,\ -0.9,\ 0.8,\ -0.4,\ 0.3,\ -0.4,\ 0.3, \\
&\qquad -0.3,\ 0.2,\ -1.2,\ 1.5,\ -1.2,\ 1.4) \\
U^{15\times 1}_{qg}(\mu_n, m_W) &= (0, 0, 0, 0, 0, 0, -1.1\cdot 10^{-6}, -4.6\cdot 10^{-10}, -1.1\cdot 10^{-6}, 0, 0, 0, \\
&\qquad -7.\cdot 10^{-7}, 5.6\cdot 10^{-10}, -7.\cdot 10^{-7})^T \\
U_{Dg}(\mu_n, m_W) &= -10^{-9} \\
U_{gg}(\mu_n, m_W) &= 1
\end{aligned} \tag{4.4}$$

The zero entries in $U^{1\times 15}_{Dq}$ and $U^{15\times 1}_{qg}$ are due to the neglect of light-quark masses.

The larger matrices are given in table form for better readability. For $U^{5\times 5}_{ll}(m_\mu, m_W)$ we have

$U^{5\times 5}_{ll}$	$C^{S\,LL}_{ee}$	$C^{S\,LL}_{\mu\mu}$	$C^{S\,LL}_{\tau\tau}$	$C^{T\,LL}_{\tau\tau}$	$C^{S\,RL}_{\tau\tau}$
$C^{S\,LL}_{ee}$	0.95	0.	0.	0.	0.
$C^{S\,LL}_{\mu\mu}$	0.	0.95	0.	0.	0.
$C^{S\,LL}_{\tau\tau}$	0.	0.	1.03	0.23	0.
$C^{T\,LL}_{\tau\tau}$	0.	0.	0.005	0.99	0.
$C^{S\,RL}_{\tau\tau}$	0.	0.	0.	0.	1.03

JHEP05(2017)117

whereas for $U_{qq}^{15\times 15}(\mu_n, m_W)$ the entries read

$U_{qq}^{15\times 15}$	$C_{dd}^{S\,LL}$	$C_{dd}^{T\,LL}$	$C_{dd}^{S\,RL}$	$C_{ss}^{S\,LL}$	$C_{ss}^{T\,LL}$	$C_{ss}^{S\,RL}$	$C_{bb}^{S\,LL}$	$C_{bb}^{T\,LL}$	$C_{bb}^{S\,RL}$	$C_{uu}^{S\,LL}$	$C_{uu}^{T\,LL}$	$C_{uu}^{S\,RL}$	$C_{cc}^{S\,LL}$	$C_{cc}^{T\,LL}$	$C_{cc}^{S\,RL}$
$C_{dd}^{S\,LL}$	1.85	0.12	0.	0.	0.	0.	0.	0.	0.	0.	0.	0.	0.	0.	0.
$C_{dd}^{T\,LL}$	0.002	0.82	0.	0.	0.	0.	0.	0.	0.	0.	0.	0.	0.	0.	0.
$C_{dd}^{S\,RL}$	0.	0.	1.85	0.	0.	0.	0.	0.	0.	0.	0.	0.	0.	0.	0.
$C_{ss}^{S\,LL}$	0.	0.	0.	1.85	0.12	0.	0.	0.	0.	0.	0.	0.	0.	0.	0.
$C_{ss}^{T\,LL}$	0.	0.	0.	0.004	0.65	0.	0.	0.	0.	0.	0.	0.	0.	0.	0.
$C_{ss}^{S\,RL}$	0.	0.	0.	0.	0.	1.85	0.	0.	0.	0.	0.	0.	0.	0.	0.
$C_{bb}^{S\,LL}$	0.	0.	0.	0.	0.	0.	1.38	0.07	0.	0.	0.	0.	0.	0.	0.
$C_{bb}^{T\,LL}$	0.	0.	0.	0.	0.	0.	0.001	0.90	0.	0.	0.	0.	0.	0.	0.
$C_{bb}^{S\,RL}$	0.	0.	0.	0.	0.	0.	0.	0.	1.38	0.	0.	0.	0.	0.	0.
$C_{uu}^{S\,LL}$	0.	0.	0.	0.	0.	0.	0.	0.	0.	1.86	−0.24	0.	0.	0.	0.
$C_{uu}^{T\,LL}$	0.	0.	0.	0.	0.	0.	0.	0.	0.	−0.004	0.81	0.	0.	0.	0.
$C_{uu}^{S\,RL}$	0.	0.	0.	0.	0.	0.	0.	0.	0.	0.	0.	1.86	0.	0.	0.
$C_{cc}^{S\,LL}$	0.	0.	0.	0.	0.	0.	0.	0.	0.	0.	0.	0.	1.81	−0.23	0.
$C_{cc}^{T\,LL}$	0.	0.	0.	0.	0.	0.	0.	0.	0.	0.	0.	0.	−0.004	0.82	0.
$C_{cc}^{S\,RL}$	0.	0.	0.	0.	0.	0.	0.	0.	0.	0.	0.	0.	0.	0.	1.81

Finally, the largest matrix is given in the form

$$U_{VV}^{16\times 16}(m_\mu, m_W) = \mathbb{I} + 10^{-2}\,\bar{U}_{VV}(m_\mu, m_W) \tag{4.5}$$

and the entries of $\bar{U}_{VV}(m_\mu, m_W)$ are given by

$\bar{U}_{VV}$	$C_{ee}^{V\,RR}$	$C_{ee}^{V\,RL}$	$C_{\mu\mu}^{V\,RR}$	$C_{\mu\mu}^{V\,RL}$	$C_{\tau\tau}^{V\,RR}$	$C_{\tau\tau}^{V\,RL}$	$C_{dd}^{V\,RR}$	$C_{dd}^{V\,RL}$	$C_{ss}^{V\,RR}$	$C_{ss}^{V\,RL}$	$C_{bb}^{V\,RR}$	$C_{bb}^{V\,RL}$	$C_{uu}^{V\,RR}$	$C_{uu}^{V\,RL}$	$C_{cc}^{V\,RR}$	$C_{cc}^{V\,RL}$
$C_{ee}^{V\,RR}$	−5.8	−0.5	−1.	−0.5	−0.3	−0.3	−0.3	−0.3	−0.3	−0.3	−0.2	−0.2	0.7	0.7	0.7	0.7
$C_{ee}^{V\,RL}$	−1.1	4.4	−1.1	−0.6	−0.3	−0.3	−0.4	−0.4	−0.4	−0.4	−0.2	−0.3	0.7	0.7	0.7	0.7
$C_{\mu\mu}^{V\,RR}$	−1.	−0.5	−5.8	−0.5	−0.3	−0.3	−0.3	−0.3	−0.3	−0.3	−0.2	−0.2	0.7	0.7	0.7	0.7
$C_{\mu\mu}^{V\,RL}$	−1.1	−0.6	−1.1	4.4	−0.3	−0.3	−0.4	−0.4	−0.4	−0.4	−0.2	−0.3	0.7	0.7	0.7	0.7
$C_{\tau\tau}^{V\,RR}$	−0.6	−0.3	−0.6	−0.3	−3.1	−0.3	−0.3	−0.3	−0.3	−0.3	−0.2	−0.2	0.6	0.6	0.6	0.6
$C_{\tau\tau}^{V\,RL}$	−0.6	−0.3	−0.6	−0.3	−0.3	2.6	−0.3	−0.3	−0.3	−0.3	−0.2	−0.2	0.6	0.6	0.6	0.6
$C_{dd}^{V\,RR}$	−0.2	−0.1	−0.2	−0.1	−0.1	−0.1	−1.2	−0.1	−0.1	−0.1	−0.1	−0.1	0.2	0.2	0.2	0.2
$C_{dd}^{V\,RL}$	−0.2	−0.1	−0.2	−0.1	−0.1	−0.1	−0.1	1.0	−0.1	−0.1	−0.1	−0.1	0.2	0.2	0.2	0.2
$C_{ss}^{V\,RR}$	−0.2	−0.1	−0.2	−0.1	−0.1	−0.1	−0.1	−0.1	−1.2	−0.1	−0.1	−0.1	0.2	0.2	0.2	0.2
$C_{ss}^{V\,RL}$	−0.2	−0.1	−0.2	−0.1	−0.1	−0.1	−0.1	−0.1	−0.1	1.0	−0.1	−0.1	0.2	0.2	0.2	0.2
$C_{bb}^{V\,RR}$	−0.2	−0.1	−0.2	−0.1	−0.1	−0.1	−0.1	−0.1	−0.1	−0.1	−0.8	−0.1	0.2	0.2	0.2	0.2
$C_{bb}^{V\,RL}$	−0.2	−0.1	−0.2	−0.1	−0.1	−0.1	−0.1	−0.1	−0.1	−0.1	−0.1	0.7	0.2	0.2	0.2	0.2
$C_{uu}^{V\,RR}$	0.5	0.2	0.5	0.2	0.2	0.2	0.2	0.2	0.2	0.2	0.2	0.2	1.7	−0.5	−0.5	−0.5
$C_{uu}^{V\,RL}$	0.5	0.2	0.5	0.2	0.2	0.2	0.2	0.2	0.2	0.2	0.2	0.2	−0.5	−2.6	−0.5	−0.5
$C_{cc}^{V\,RR}$	0.5	0.2	0.5	0.2	0.2	0.2	0.2	0.2	0.2	0.2	0.2	0.2	−0.5	−0.5	1.7	−0.5
$C_{cc}^{V\,RL}$	0.5	0.2	0.5	0.2	0.2	0.2	0.2	0.2	0.2	0.2	0.2	0.2	−0.5	−0.5	−0.5	−2.6

Of course, it is no problem to change the high scale from m_W to another scale Λ, as long as $m_W \geq \Lambda \gg m_b$.

5 Phenomenological analysis

In this section we use the concepts presented previously for a phenomenological analysis.[6] For this purpose, we assume that the Wilson coefficients (which are generated by some underlying NP theory above the EWSB scale) are given at $\Lambda = m_W$. In a first step, we use the RGEs presented in section 4 to evolve the Wilson coefficients from the high scale m_W to the

[6] Parts of these results were already presented in the proceedings [58].

JHEP05(2017)117

low experimental scale (namely μ_n and m_μ, respectively). At the low scale, the predicted rates are then confronted with the experimental limits. This results in constraints on the various Wilson coefficients at the high scale. Due to mixing effects in the RGE, Wilson coefficients that are zero at the high scale can be non-zero at the low scale. Hence we are able to place bounds on coefficients which would be unconstrained if loop effects were disregarded.

In this analysis, we use the following current experimental limits:

$$\mathrm{Br}\left(\mu^+ \to e^+\gamma\right) \leq 4.2 \times 10^{-13}\,, \tag{5.1}$$

$$\mathrm{Br}\left(\mu^+ \to e^+e^-e^+\right) \leq 1.0 \times 10^{-12}\,, \tag{5.2}$$

$$\mathrm{Br}^{\mathrm{Au}}_{\mu\to e} \leq 7.0 \times 10^{-13}\,, \tag{5.3}$$

from the MEG [1, 2], SINDRUM [3] and SINDRUM II [4] collaborations, respectively. In addition, the following future experimental limits

$$\mathrm{Br}\left(\mu^+ \to e^+\gamma\right) \leq 4.0 \times 10^{-14}\,, \tag{5.4}$$

$$\mathrm{Br}\left(\mu^+ \to e^+e^-e^+\right) \leq 5.0 \times 10^{-15}\,, \tag{5.5}$$

$$\mathrm{Br}^{\mathrm{Al}}_{\mu\to e} \leq 1.0 \times 10^{-16}\,, \tag{5.6}$$

from the MEG II [5], Mu3e [6] and Mu2e/COMET [8–10] are considered.

Let us start by assuming that at the high scale m_W only one Wilson coefficient at a time is non-zero. The corresponding bounds on the coefficients are shown in table 3 both for the current and for the future experimental limits. Note that for $\mu \to 3e$ we did not take into account efficiency corrections due to cuts on the transverse momentum applied in the experimental analysis. These corrections are in general small for 4-fermion operators but significantly reduce the sensitivity to the dipole operator. From table 3 we can infer the following general structure of these limits:

- Experimental bounds on the direct $\mu \to e\gamma$ transition represent a powerful tool to test the Wilson coefficients of the dipole operator. Furthermore, the impact of mixing effects originating from some scalar and tensor operators can also be examined with high precision. However, future prospects for nuclear conversion are so good, that it could overtake the direct $\mu \to e\gamma$ limits. The only (numerically accidental) exception is represented by $C^S_{\mu\mu}$, that will be still better constrained by the next generation of $\mu \to e\gamma$ experiments.

- A $\mu \to 3e$ experiment is the most powerful tool to explore μ-e-e-e Wilson coefficients of four fermion operators, regardless of the Dirac structure of the operator. This is mainly due to the fact that such interactions produce the $\mu \to 3e$ decay already at the tree level (see eq. (3.2)) while it enters all other processes only via loop effects.

- As expected, $\mu \to e$ conversion is the most sensitive experimental framework to explore the set of operators including quarks (with exception of current limits on $C^T_{cc/bb}$, the Wilson coefficients of tensor operators) and gluons. However, it also appears to be the best setup to study any kind of vector interaction (with the exception of the aforementioned C^V_{ee} operators, for which $\mu \to 3e$ represents the golden channel). This is mostly due to notable RGE effects in the vector operator mixing matrix.

JHEP05(2017)117

	$\mathrm{Br}\,(\mu^+ \to e^+\gamma)$		$\mathrm{Br}\,(\mu^+ \to e^+e^-e^+)$		$\mathrm{Br}^{\mathrm{Au/Al}}_{\mu\to e}$	
	$4.2 \cdot 10^{-13}$	$4.0 \cdot 10^{-14}$	$1.0 \cdot 10^{-12}$	$5.0 \cdot 10^{-15}$	$7.0 \cdot 10^{-13}$	$1.0 \cdot 10^{-16}$
C_L^D	$1.0 \cdot 10^{-8}$	$3.1 \cdot 10^{-9}$	$2.0 \cdot 10^{-7}$	$1.4 \cdot 10^{-8}$	$2.0 \cdot 10^{-7}$	$2.9 \cdot 10^{-9}$
$C_{ee}^{S\,LL}$	$4.8 \cdot 10^{-5}$	$1.5 \cdot 10^{-5}$	$8.1 \cdot 10^{-7}$	$5.8 \cdot 10^{-8}$	$1.4 \cdot 10^{-3}$	$2.1 \cdot 10^{-5}$
$C_{\mu\mu}^{S\,LL}$	$2.3 \cdot 10^{-7}$	$7.2 \cdot 10^{-8}$	$4.6 \cdot 10^{-6}$	$3.3 \cdot 10^{-7}$	$7.1 \cdot 10^{-6}$	$1.0 \cdot 10^{-7}$
$C_{\tau\tau}^{S\,LL}$	$1.2 \cdot 10^{-6}$	$3.7 \cdot 10^{-7}$	$2.4 \cdot 10^{-5}$	$1.7 \cdot 10^{-6}$	$2.4 \cdot 10^{-5}$	$3.5 \cdot 10^{-7}$
$C_{\tau\tau}^{T\,LL}$	$2.9 \cdot 10^{-9}$	$9.0 \cdot 10^{-10}$	$5.7 \cdot 10^{-8}$	$4.1 \cdot 10^{-9}$	$5.9 \cdot 10^{-8}$	$8.5 \cdot 10^{-10}$
$C_{\tau\tau}^{S\,LR}$	$9.4 \cdot 10^{-6}$	$2.9 \cdot 10^{-6}$	$1.8 \cdot 10^{-4}$	$1.3 \cdot 10^{-5}$	$1.9 \cdot 10^{-4}$	$2.7 \cdot 10^{-6}$
$C_{bb}^{S\,LL}$	$2.8 \cdot 10^{-6}$	$8.6 \cdot 10^{-7}$	$5.4 \cdot 10^{-5}$	$3.8 \cdot 10^{-6}$	$9.0 \cdot 10^{-7}$	$1.2 \cdot 10^{-8}$
$C_{bb}^{T\,LL}$	$2.1 \cdot 10^{-9}$	$6.4 \cdot 10^{-10}$	$4.1 \cdot 10^{-8}$	$2.9 \cdot 10^{-9}$	$4.2 \cdot 10^{-8}$	$6.0 \cdot 10^{-10}$
$C_{bb}^{S\,LR}$	$1.7 \cdot 10^{-5}$	$5.1 \cdot 10^{-6}$	$3.2 \cdot 10^{-4}$	$2.3 \cdot 10^{-5}$	$9.1 \cdot 10^{-7}$	$1.2 \cdot 10^{-8}$
$C_{cc}^{S\,LL}$	$1.4 \cdot 10^{-6}$	$4.4 \cdot 10^{-7}$	$2.8 \cdot 10^{-5}$	$2.0 \cdot 10^{-6}$	$1.8 \cdot 10^{-7}$	$2.4 \cdot 10^{-9}$
$C_{cc}^{T\,LL}$	$3.5 \cdot 10^{-9}$	$1.1 \cdot 10^{-9}$	$6.8 \cdot 10^{-8}$	$4.8 \cdot 10^{-9}$	$6.6 \cdot 10^{-8}$	$9.5 \cdot 10^{-10}$
$C_{cc}^{S\,LR}$	$1.2 \cdot 10^{-5}$	$3.6 \cdot 10^{-6}$	$2.3 \cdot 10^{-4}$	$1.6 \cdot 10^{-5}$	$1.8 \cdot 10^{-7}$	$2.4 \cdot 10^{-9}$
$C_{ee}^{V\,RR}$	$3.0 \cdot 10^{-5}$	$9.4 \cdot 10^{-6}$	$2.1 \cdot 10^{-7}$	$1.5 \cdot 10^{-8}$	$2.1 \cdot 10^{-6}$	$3.5 \cdot 10^{-8}$
$C_{ee}^{V\,RL}$	$6.7 \cdot 10^{-5}$	$2.1 \cdot 10^{-5}$	$2.6 \cdot 10^{-7}$	$1.9 \cdot 10^{-8}$	$4.0 \cdot 10^{-6}$	$6.7 \cdot 10^{-8}$
$C_{\mu\mu}^{V\,RR}$	$3.0 \cdot 10^{-5}$	$9.4 \cdot 10^{-6}$	$1.6 \cdot 10^{-5}$	$1.1 \cdot 10^{-6}$	$2.1 \cdot 10^{-6}$	$3.5 \cdot 10^{-8}$
$C_{\mu\mu}^{V\,RL}$	$2.7 \cdot 10^{-5}$	$8.5 \cdot 10^{-6}$	$2.9 \cdot 10^{-5}$	$2.0 \cdot 10^{-6}$	$4.0 \cdot 10^{-6}$	$6.6 \cdot 10^{-8}$
$C_{\tau\tau}^{V\,RR}$	$1.0 \cdot 10^{-4}$	$3.2 \cdot 10^{-5}$	$5.3 \cdot 10^{-5}$	$3.8 \cdot 10^{-6}$	$4.8 \cdot 10^{-6}$	$7.9 \cdot 10^{-8}$
$C_{\tau\tau}^{V\,RL}$	$1.2 \cdot 10^{-4}$	$3.6 \cdot 10^{-5}$	$5.1 \cdot 10^{-5}$	$3.6 \cdot 10^{-6}$	$4.6 \cdot 10^{-6}$	$7.6 \cdot 10^{-8}$
$C_{bb}^{V\,RR}$	$3.5 \cdot 10^{-4}$	$1.1 \cdot 10^{-4}$	$6.7 \cdot 10^{-5}$	$4.8 \cdot 10^{-6}$	$6.0 \cdot 10^{-6}$	$1.0 \cdot 10^{-7}$
$C_{bb}^{V\,RL}$	$5.3 \cdot 10^{-4}$	$1.6 \cdot 10^{-4}$	$6.6 \cdot 10^{-5}$	$4.7 \cdot 10^{-6}$	$6.0 \cdot 10^{-6}$	$9.9 \cdot 10^{-8}$
$C_{cc}^{V\,RR}$	$8.1 \cdot 10^{-5}$	$2.5 \cdot 10^{-5}$	$2.3 \cdot 10^{-5}$	$1.6 \cdot 10^{-6}$	$2.1 \cdot 10^{-6}$	$3.4 \cdot 10^{-8}$
$C_{cc}^{V\,RL}$	$6.7 \cdot 10^{-5}$	$2.1 \cdot 10^{-5}$	$2.4 \cdot 10^{-5}$	$1.7 \cdot 10^{-6}$	$2.1 \cdot 10^{-6}$	$3.5 \cdot 10^{-8}$
C_{gg}^{L}	N/A	N/A	N/A	N/A	$6.2 \cdot 10^{-3}$	$8.1 \cdot 10^{-5}$

Table 3. Limits on the various coefficients $C_i(m_W)$ from current and future experimental constraints, assuming that (at the high scale m_W) only one coefficient at a time is non-vanishing and not including operator-dependent efficiency corrections.

Concerning, $\mu \to e$ conversion it is important to keep in mind that we chose for the constraints in table 3 a chiral basis, i.e. we worked with left- and right-handed fields. However, for Wilson coefficients given at the low experimental scale, the $\mu \to e$ conversion rate is only sensitive to operators with vector or scalar currents on the quark side, but not to operators with axial-vector or pseudo-scalar currents. Therefore, it is informative to switch the basis and consider operators with scalar (vector) and pseudo-scalar (axial-vector) currents instead:

$$C_{ff}^{XS} = \frac{C_{ff}^{SXR} + C_{ff}^{SXL}}{2}, \qquad C_{ff}^{XV} = \frac{C_{ff}^{VXR} + C_{ff}^{VXL}}{2}, \tag{5.7}$$

$$C_{ff}^{XP} = \frac{C_{ff}^{SXR} - C_{ff}^{SXL}}{2}, \qquad C_{ff}^{XA} = \frac{C_{ff}^{VXR} - C_{ff}^{VXL}}{2}, \tag{5.8}$$

JHEP05(2017)117

	$\mathrm{Br}\,(\mu^+ \to e^+\gamma)$		$\mathrm{Br}\,(\mu^+ \to e^+e^-e^+)$		$\mathrm{Br}_{\mu\to e}^{\mathrm{Au/Al}}$	
	$4.2 \cdot 10^{-13}$	$4.0 \cdot 10^{-14}$	$1.0 \cdot 10^{-12}$	$5.0 \cdot 10^{-15}$	$7.0 \cdot 10^{-13}$	$1.0 \cdot 10^{-16}$
C_{bb}^{LP}	$4.7 \cdot 10^{-6}$	$1.5 \cdot 10^{-6}$	$9.3 \cdot 10^{-5}$	$6.6 \cdot 10^{-6}$	$9.6 \cdot 10^{-5}$	$1.4 \cdot 10^{-6}$
C_{bb}^{LS}	$6.7 \cdot 10^{-6}$	$2.1 \cdot 10^{-6}$	$1.3 \cdot 10^{-4}$	$9.2 \cdot 10^{-6}$	$9.1 \cdot 10^{-7}$	$1.2 \cdot 10^{-8}$
C_{cc}^{LP}	$2.6 \cdot 10^{-6}$	$7.9 \cdot 10^{-7}$	$5.0 \cdot 10^{-5}$	$3.5 \cdot 10^{-6}$	$5.0 \cdot 10^{-5}$	$7.1 \cdot 10^{-7}$
C_{cc}^{LS}	$3.3 \cdot 10^{-6}$	$1.0 \cdot 10^{-6}$	$6.4 \cdot 10^{-5}$	$4.5 \cdot 10^{-6}$	$1.8 \cdot 10^{-7}$	$2.4 \cdot 10^{-9}$
C_{dd}^{RA}	$2.9 \cdot 10^{-4}$	$8.8 \cdot 10^{-5}$	$3.9 \cdot 10^{-3}$	$2.8 \cdot 10^{-4}$	$6.6 \cdot 10^{-7}$	$1.4 \cdot 10^{-8}$
C_{dd}^{RV}	$1.4 \cdot 10^{-3}$	$4.3 \cdot 10^{-4}$	$4.5 \cdot 10^{-5}$	$3.2 \cdot 10^{-6}$	$7.2 \cdot 10^{-9}$	$1.5 \cdot 10^{-10}$
C_{ss}^{RA}	$2.9 \cdot 10^{-4}$	$8.8 \cdot 10^{-5}$	$3.9 \cdot 10^{-3}$	$2.8 \cdot 10^{-4}$	$6.5 \cdot 10^{-4}$	$1.1 \cdot 10^{-5}$
C_{ss}^{RV}	$1.4 \cdot 10^{-3}$	$4.3 \cdot 10^{-4}$	$4.5 \cdot 10^{-5}$	$3.2 \cdot 10^{-6}$	$4.1 \cdot 10^{-6}$	$6.8 \cdot 10^{-8}$
C_{bb}^{RA}	$4.2 \cdot 10^{-4}$	$1.3 \cdot 10^{-4}$	$6.5 \cdot 10^{-3}$	$4.6 \cdot 10^{-4}$	$1.3 \cdot 10^{-3}$	$2.2 \cdot 10^{-5}$
C_{bb}^{RV}	$2.1 \cdot 10^{-3}$	$6.4 \cdot 10^{-4}$	$6.7 \cdot 10^{-5}$	$4.7 \cdot 10^{-6}$	$6.0 \cdot 10^{-6}$	$1.0 \cdot 10^{-7}$
C_{uu}^{RA}	$7.2 \cdot 10^{-5}$	$2.2 \cdot 10^{-5}$	$9.8 \cdot 10^{-4}$	$6.9 \cdot 10^{-5}$	$3.8 \cdot 10^{-7}$	$7.2 \cdot 10^{-9}$
C_{uu}^{RV}	$7.7 \cdot 10^{-4}$	$2.4 \cdot 10^{-4}$	$2.3 \cdot 10^{-5}$	$1.6 \cdot 10^{-6}$	$8.3 \cdot 10^{-9}$	$1.6 \cdot 10^{-10}$
C_{cc}^{RA}	$7.3 \cdot 10^{-5}$	$2.3 \cdot 10^{-5}$	$1.0 \cdot 10^{-3}$	$7.1 \cdot 10^{-5}$	$1.7 \cdot 10^{-4}$	$2.8 \cdot 10^{-6}$
C_{cc}^{RV}	$7.8 \cdot 10^{-4}$	$2.4 \cdot 10^{-4}$	$2.3 \cdot 10^{-5}$	$1.6 \cdot 10^{-6}$	$2.1 \cdot 10^{-6}$	$3.5 \cdot 10^{-8}$

Table 4. Limits on the Wilson coefficients (given at the scale m_W) with scalar (vector) and pseudo-scalar (axial-vector) currents from current and future experimental constraints, assuming that only one coefficient at a time is non-vanishing at the high scale.

where $X \in \{L, R\}$ and $f \in \{u, c, d, s, b, e, \mu, \tau\}$. In a simplistic tree-level approach, $\mu \to e$ conversion is not sensitive to C_{ff}^{XA} and C_{ff}^{XP}. However, the remarkable outcome is that axial-vector operators mix into vector operators. This results in strong bounds from $\mu \to e$ conversion in nuclei once the Wilson coefficients are evaluated at a scale higher than the experimental scale. Therefore, the common preconceptions that $\mu \to e$ conversion is not sensitive to axial-vector currents is not true anymore once loop effects are taken into account. The corresponding results are presented in table 4. In order to understand how the parity-selection rules work for the vectorial lepton-quark and lepton-tau operators, in figure 1 we show the Feynman diagrams of their mixing at the one-loop level.

First, vectorial operators do not receive contribution from the diagrams in figure 1b (they vanish when the wave-function renormalisation is included). After, we remark that the penguin diagram in figure 1a generates operators in which the flavour conserving current has a vectorial structure, i.e. vector-vector and axial-vector operators. Then, from the contribution of the diagrams in figure 1c one obtains a "maximally flipped" operatorial mixing: axial-axial into vector-vector, axial-vector into vector-axial, vector-axial into axial-vector and vector-vector into axial-axial. By combining the contributions, the parity selection rules work as follows: vector-vector and axial-axial operators mix into vector-vector (with the contribution from the penguin diagram), axial-vector mixes into vector-axial, axial-vector and vector-axial mix into axial-vector (with the contribution from the penguin diagram), and vector-vector mixes into axial-axial. These results have been discussed also by previous literature [59, 60].

JHEP05(2017)117

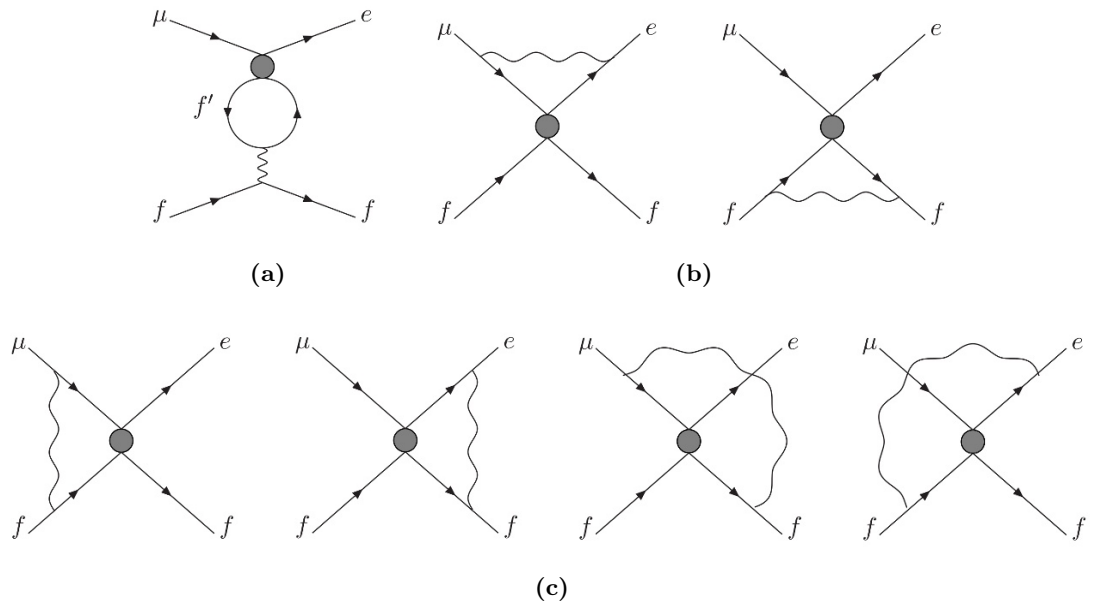

Figure 1. One-loop Feynman diagrams for the mixing of the four-fermion lepton-quark and lepton-tau operators.

In a next step let us compare the exploring power of current and future $\mu \to e\gamma$, $\mu \to 3e$ and $\mu \to e$ conversion experiments by directly relating the branching-ratio limits that are needed for the various processes to achieve a particular bound on a Wilson coefficient. For illustrative purposes, we single out two coefficients namely $C_{\mu\mu}^{S\,LL}$ and $C_{ee}^{V\,RR}$. In figure 2, the current and future branching ratio for $\mu \to e\gamma$ and $\mu \to 3e$ experiments are compared to the future $\mu N \to eN$ prospects (where N is an aluminium nucleus).

Starting with the upper panel, the horizontal dashed red line for example indicates that a rather modest limit $\mathrm{Br}(\mu \to e\gamma) \lesssim 10^{-12}$ is as constraining on $C_{\mu\mu}^{S\,LL}$ as the future Mu3e limit $\mathrm{Br}(\mu \to 3e) < 5 \times 10^{-15}$. In order for muon conversion to be more constraining a limit of $\mathrm{Br}(\mu N \to eN) < 10^{-15}$ would be required. This is indicated by the vertical dashed red line. The future MEG II experiment will place the strongest limit on $C_{\mu\mu}^{S\,LL}$ unless the COMET or Mu2e experiments improve their expected limit to reach at least $\mathrm{Br}(\mu N \to eN) < 5 \times 10^{-17}$. For this specific operator Mu3e will have less of an impact.

From the lower panel, we infer that the future Mu3e experiment will deliver the best bound on $C_{ee}^{V\,RR}$. In order to perform with similar standards, the COMET and Mu2e experiments will have to obtain a limit of $\mathrm{Br}(\mu N \to eN) < 2 \times 10^{-17}$. Instead, in this specific context, the MEG II experiment will exhibit a generally weak sensitivity, orders of magnitude below the capability of the other experiments.

So far we have considered a scenario where only one coefficient at a time is non-vanishing at the high scale. Now, let us extend the previous results by assuming two Wilson coefficients are non-vanishing. For this purpose, we generated plots in which the parameter space is analysed in light of current and future experimental limits for all three processes. For a better understanding, we display them in a (pseudo-)logarithmic scale.

JHEP05(2017)117

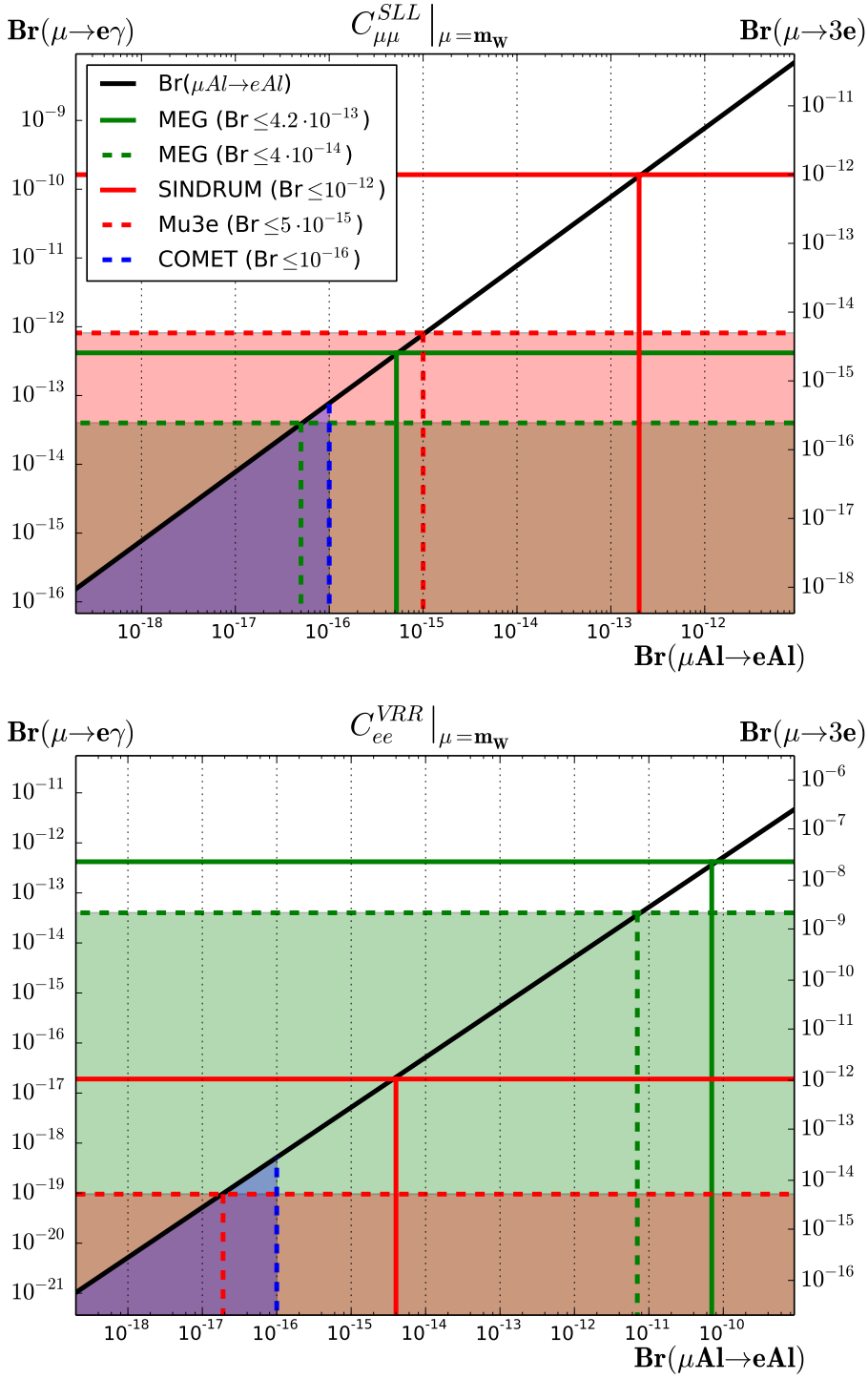

Figure 2. Br($\mu \to e\gamma$) (Br($\mu \to 3e$)) plotted on the left (right) y-axis against Br($\mu N \to eN$) for a fixed value of $C_{\mu\mu}^{S\,LL}$ (upper panel) and $C_{ee}^{V\,RR}$ (lower panel) given at the scale $\mu = m_W$. Current and future experimental limits are displayed.

JHEP05(2017)117

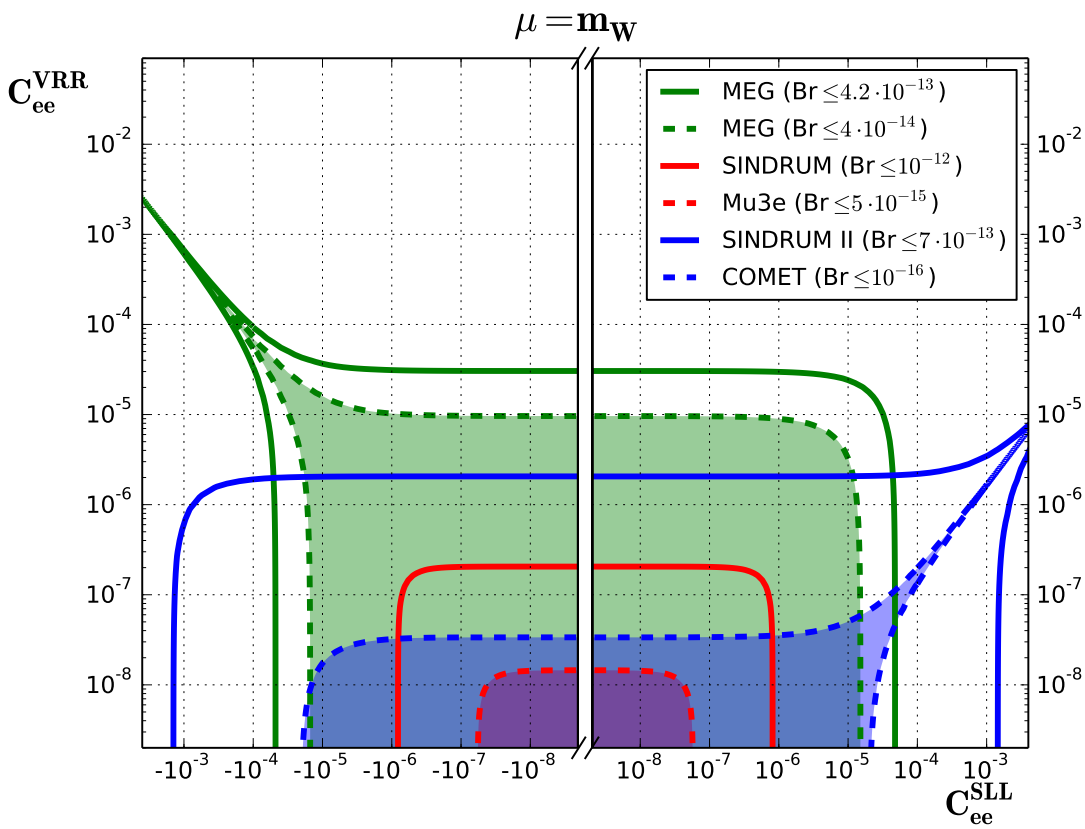

Figure 3. Allowed regions in the $C_{ee}^{S\,LL} - C_{ee}^{V\,RR}$ plane from $\mu \to e\gamma$ (green), $\mu \to 3e$ (red) and $\mu \to e$ conversion (blue) for current (straight) and future (dashed) experimental limits.

In figure 3 we show the allowed regions in the $C_{ee}^{S\,LL} - C_{ee}^{V\,RR}$ plane (given at the scale m_W). Comparing current (solid lines) and future (dashed lines) limits on $\mu \to e\gamma$ (in green) and $\mu \to e$ conversion (in blue) to those of $\mu \to 3e$ (in red) indicate that $\mu \to 3e$ experiments are most sensitive to these Wilson coefficients. It is also interesting to note that the other experimental setups could be blind to specific regions in parameter space where cancellations occur, while this is never the case for $\mu \to 3e$. This is mostly due to the fact that these operators trigger $\mu \to 3e$ already at the tree-level while they give rise to the other processes only via mixing effects.

In figure 4 we show an analogous plot for the Wilson coefficients $C_{\tau\tau}^{V\,RL}$ and $C_{bb}^{V\,RR}$. In this case, $\mu \to e$ conversion experiments display a superior capability to probe vectorial four-fermion operators, as previously discussed. Even the new Mu3e experiment will be just a little better than the current $\mu \to e$ conversion limit established by SINDRUM II more than a decade ago. However, the plot demonstrates an interesting complementarity among various experiments: assuming that the underlying theory produces a cancellation both in $\mu \to e$ conversion and $\mu \to 3e$, then $\mu \to e\gamma$ experiments will provide a complementary limit, finally closing the allowed region of the parameter space.

In figure 5, we focus on the coefficients C_L^D and $C_{ee}^{V\,RR}$. Here, the current limit on the C_L^D coefficient comes from the MEG experiment, and the future one will be set by the $\mu \to e$ conversion. On the other hand, the past SINDRUM and future Mu3e experiments

JHEP05(2017)117

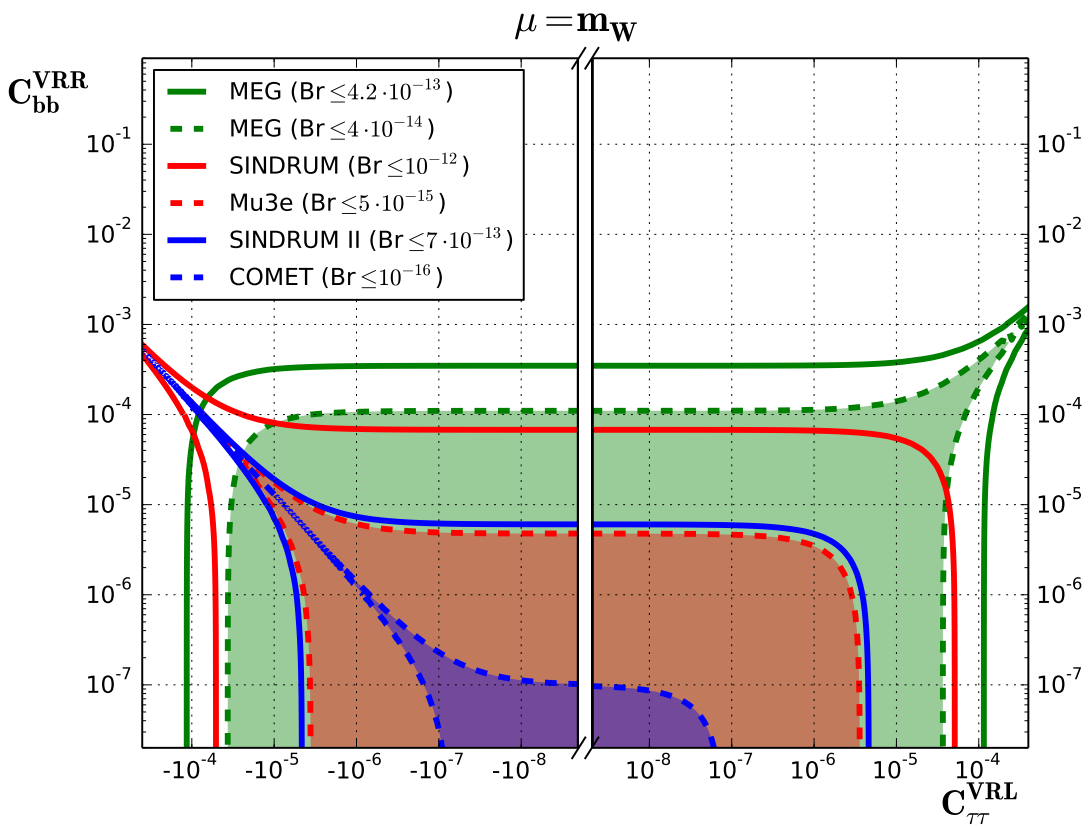

Figure 4. Allowed regions in the $C_{\tau\tau}^{V\,RL} - C_{bb}^{V\,RR}$ plane from $\mu \to e\gamma$ (green), $\mu \to 3e$ (red) and $\mu \to e$ conversion (blue) for current (straight) and future (dashed) experimental limits.

give the most significant limits on the coefficient $C_{ee}^{V\,RR}$. However, especially in the corners of the parameter space where there are potential cancellations between the contributions from C_L^D and $C_{ee}^{V\,RR}$, an interesting interplay between the observables implies that all of the future experimental limits are useful to ensure that no blind spots in parameter space exist.

With figure 6 we conclude our review on correlations, by showing the allowed regions in the $C_L^D - C_{bb}^{S\,LR}$ plane. The first information one obtains from the plot is that for this case $\mu \to 3e$ experiments are less constraining than the other two experimental options. In the long term, $\mu \to e$ conversion will set the best limits on each Wilson coefficient separately. However, there is a big portion of the parameter space where a cancellation in $\mu \to e$ conversion occurs. Results from MEG II will play an important role to cover this region.

Of course, our choice of combinations for the free parameters is far from being exhaustive. However, the main message is that the interplay between the various experiments is crucial to cover all corners of the parameter space, also the ones in which cancellation can result in blind spots for one or even two specific experiments.

Obviously, it is easily possible to investigate scenarios where several Wilson coefficients are present at the large scale. A very efficient way to determine the impact of the experimental limits on a particular BSM model is to obtain the Wilson coefficients at the weak scale through matching and then use the RGE. A reasonable approximation for the RGE can be obtained by using the numerical evolution matrices given in section 4. This deter-

JHEP05(2017)117

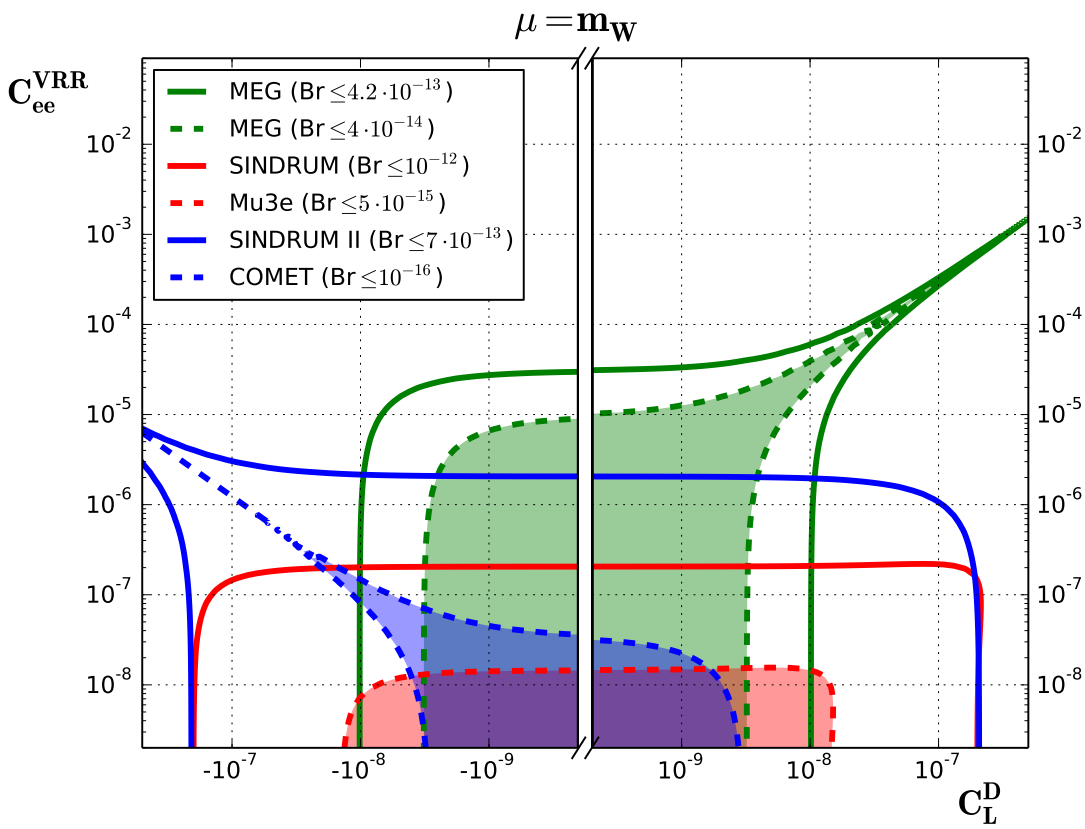

Figure 5. Allowed regions in the $C_L^D - C_{ee}^{V\,RR}$ plane from $\mu \to e\gamma$ (green), $\mu \to 3e$ (red) and $\mu \to e$ conversion (blue) for current (straight) and future (dashed) experimental limits.

mines the coefficients entering eqs. (3.1), (3.2) and (3.5) and, hence, immediately indicates whether for the chosen parameters the model is still allowed or ruled out.

6 Conclusions and outlook

In this article, we have provided RGE improved predictions for the three $\mu \to e$ processes $\mu \to e\gamma$, $\mu \to 3e$ and $\mu \to e$ conversion in nuclei. Working within the effective theory valid below the EW breaking scale, we have computed the complete one-loop anomalous dimensions for the contributing dim-6 operators taking into account QED and QCD effects. In addition, we have included the leading two-loop QED effects for the mixing of vector operators into the dipole operators and recalled the formula for the $\mu \to e\gamma$, $\mu \to 3e$ and $\mu \to e$ conversion rates.

Our $O(\alpha_{(s)})$ RGE is renormalisation-scheme independent and can be used for the evolution of the Wilson coefficients from any matching scale $\Lambda \lesssim m_W$ to the scale of the experiments, after a $O(\alpha_{(s)}^0)$ matching has been performed. If the NP theory is realised well above the EWSB scale, this NP theory first has to be matched to the SMEFT and the RGE within the SMEFT [25, 26] has to be applied for the evolution from Λ to m_W. If a NP theory is realised below or not too far above the EW scale it is sufficient to match it directly to our Lagrangian and use the RGE discussed in this paper.

JHEP05(2017)117

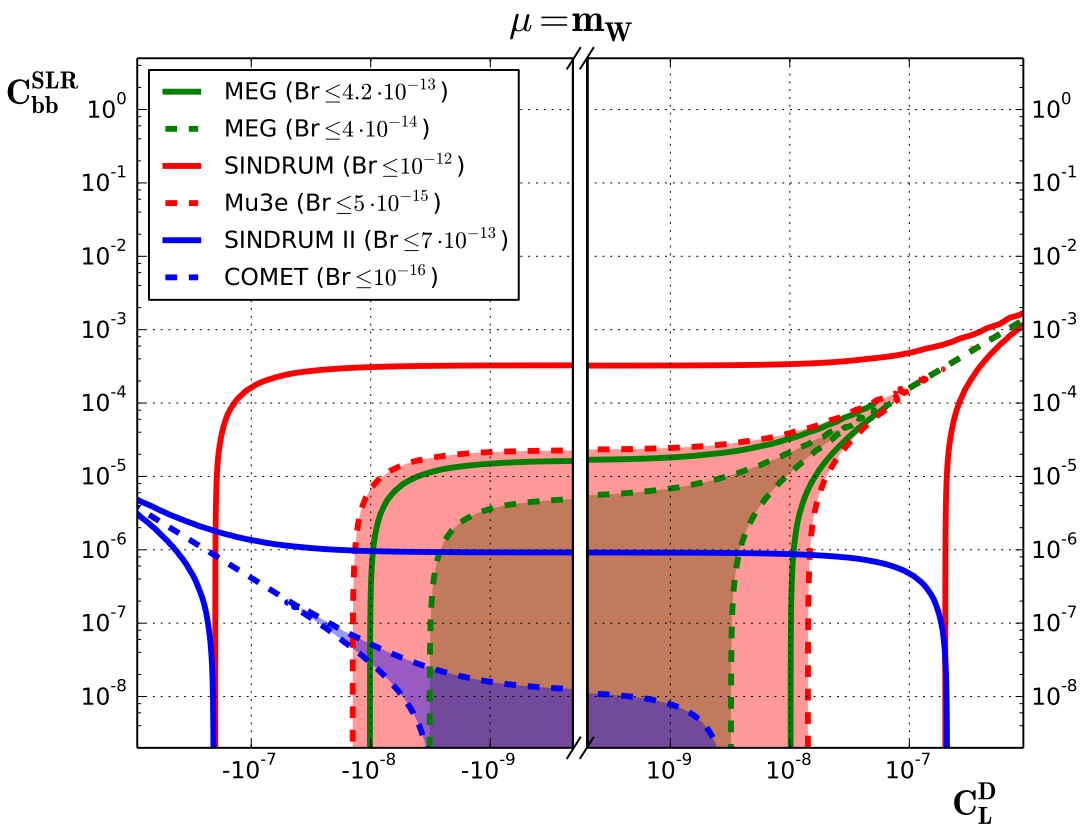

Figure 6. Allowed regions in the $C_L^D - C_{ee}^{V\,RR}$ plane from $\mu \to e\gamma$ (green), $\mu \to 3e$ (red) and $\mu \to e$ conversion (blue) for current (straight) and future (dashed) experimental limits.

In our phenomenological analysis we have provided a numerical solution for the RGE. In a second step, we have summarised the resulting bounds on the Wilson coefficients (given at the scale m_W) under the assumption that only one Wilson coefficient at a time is non-zero (see tables 3 and 4). Afterwards, we have shown the complementary of the three $\mu \to e$ processes by pointing out the capability of covering regions of parameter space which would be blind spots for a single process.

The limits presented in this paper should be interpreted in light of the fact that they have been obtained under several simplifying assumptions. In particular, obtaining more accurate predictions for the rates as a function of the Wilson coefficients is not the main aim of including RGE contributions. More importantly, one obtains quantitatively new effects. For example 4-fermion vector operators with b, c or s quarks, which do not enter any of these processes directly, mix into contributing operators resulting in stringent constraints. Furthermore, operators with axial-vector currents, which do not enter $\mu \to e$ conversion at tree-level, mix into contributing vector operators. Therefore, many more correlations among the $\mu \to e$ processes are present once the RGE effects are taken into account.

The future prospects for observables involving $\mu \to e$ transitions are intriguing. MEG II will improve the sensitivity on $\mu \to e\gamma$ by nearly an order of magnitude, while the existing bounds on $\mu \to 3e$ and $\mu \to e$ conversion could even improve by four orders of magnitude.

JHEP05(2017)117

Interestingly, if $\mu \to e$ conversion managed to improve further to Br $\sim 10^{-18}$ it could be competitive with $\mu \to 3e$ even for vector operators involving three electrons once loop effects are taken into account. Furthermore, the search for $\mu \to e$ transitions in Kaon decays like $K \to \mu e$ or $K \to \pi\mu e$ (see [61] for a recent account) but also in LFV B (see for example [62, 63]) and tau decays (see for example [18, 64–66]) can give complementary information. While, in our EFT defined below the EW scale, these processes are completely unrelated this situation would change once flavour symmetries are involved or if EW matching effects are considered.

Acknowledgments

AC is supported by an Ambizione Grant (PZ00P2_154834) of the Swiss National Science Foundation (SNSF). GMP is supported by the SNSF under contract 200021_160156. GMP is thankful to Christoph Gnendiger for the crosscheck of the anomalous dimensions of appendix A.

A Anomalous dimensions

In this appendix, the running of the coefficients of the operators listed in eqs. (2.2)–(2.8) are presented. We use

$$\dot{C} \equiv (4\pi)\,\mu \frac{\mathrm{d}}{\mathrm{d}\mu}\, C \tag{A.1}$$

and $C_F = (N_c^2 - 1)/(2N_c)$ with N_c the number of colours. $Q_l = -1$, $Q_u = 2/3$, $Q_d = -1/3$ are the charges associated to leptons, u-type and d-type quarks, respectively. The corresponding equations for the chirality-flipped operators can be obtained form the label interchange $R \leftrightarrow L$. In our computation, the covariant derivative is defined according to the convention of `FeynRules v2.3`: $D_\mu\phi = \partial_\mu\phi - i g_s G^a_\mu T_a \phi$ and $D_\mu\phi = \partial_\mu\phi - ieQ_\phi A_\mu \phi$, where ϕ is a generic field, G^a_μ and A_μ are the gluon and photon gauge field respectively, T_a is the colour matrix and Q_ϕ is the electromagnetic charge associated to the field ϕ.

The coefficient of the dipole operator runs according to

$$\begin{aligned}
\dot{C}^D_L = {} & 16\,\alpha_e\, Q_l^2 C^D_L - \frac{Q_l}{(4\pi)}\frac{m_e}{m_\mu} C^{S\,LL}_{ee} - \frac{Q_l}{(4\pi)} C^{S\,LL}_{\mu\mu} \\
& + \sum_h \frac{8Q_h}{(4\pi)}\frac{m_h}{m_\mu} N_{c,h}\, C^{T\,LL}_{hh}\, \Theta(\mu - m_h) \\
& - \frac{\alpha_e Q_l^3}{(4\pi)^2}\left(\frac{116}{9} C^{V\,RR}_{ee} + \frac{116}{9} C^{V\,RR}_{\mu\mu} - \frac{122}{9} C^{V\,RL}_{\mu\mu} - \left(\frac{50}{9} + 8\,\frac{m_e}{m_\mu}\right) C^{V\,RL}_{ee}\right) \\
& - \sum_h \frac{\alpha_e}{(4\pi)^2}\left(6Q_h^2 Q_l + \frac{4Q_h Q_l^2}{9}\right) N_{c,h}\, C^{V\,RR}_{hh}\, \Theta(\mu - m_h) \\
& - \sum_h \frac{\alpha_e}{(4\pi)^2}\left(-6Q_h^2 Q_l + \frac{4Q_h Q_l^2}{9}\right) N_{c,h}\, C^{V\,RL}_{hh}\, \Theta(\mu - m_h) \\
& - \sum_h \frac{\alpha_e}{(4\pi)^2}\, 4Q_h^2 Q_l N_{c,h} \frac{m_h}{m_\mu} C^{S\,LR}_{hh}\, \Theta(\mu - m_h)\,,
\end{aligned} \tag{A.2}$$

JHEP05(2017)117

where the sums run over $h \in \{\tau, d, s, b, u, c\}$ with $N_{c,\tau} = 1$ and $N_{c,q} = N_c$, respectively. The terms in the last four lines are due to two-loop contributions from vector operators (or scalar operators that can be Fierz-transformed into vector operators) to the anomalous dimension of Q_L^D.

The running of the whole set of vector operators is given by the following two equations:

$$\dot{C}_{ff}^{V\,RR} = \frac{4\,\alpha_e}{3} Q_f \left(2Q_l \sum_{\ell=e,\mu} C_{\ell\ell}^{V\,RR} + Q_l C_{\tau\tau}^{V\,RR} + Q_l \sum_l C_{ll}^{V\,RL} \right.$$
$$\left. + N_c \sum_q Q_q \left(C_{qq}^{V\,RR} + C_{qq}^{V\,RL} \right) + 9 Q_l C_{ff}^{V\,RR} \right), \tag{A.3}$$

$$\dot{C}_{ff}^{V\,RL} = \frac{4\,\alpha_e}{3} Q_f \left(2Q_l \sum_{\ell=e,\mu} C_{\ell\ell}^{V\,RR} + Q_l C_{\tau\tau}^{V\,RR} + Q_l \sum_l C_{ll}^{V\,RL} \right.$$
$$\left. + N_c \sum_q Q_q \left(C_{qq}^{V\,RR} + C_{qq}^{V\,RL} \right) - 9 Q_l C_{ff}^{V\,RL} \right), \tag{A.4}$$

where $\ell \in \{e, \mu\}$, $l \in \{e, \mu, \tau\}$ and $q \in \{d, s, b, u, c\}$.

The running of the leptonic scalar and tensorial operators is summarised by the following equations:

$$\dot{C}_{\ell\ell}^{S\,LL} = 12\,\alpha_e\, Q_l^2 C_{\ell\ell}^{S\,LL} \qquad \text{for } \ell \in \{e, \mu\}, \tag{A.5}$$
$$\dot{C}_{\tau\tau}^{S\,LL} = -12\,\alpha_e\, Q_l^2 \left(C_{\tau\tau}^{S\,LL} + 8 C_{\tau\tau}^{T\,LL} \right), \tag{A.6}$$
$$\dot{C}_{\tau\tau}^{S\,LR} = -12\,\alpha_e\, Q_l^2 C_{\tau\tau}^{S\,LR}, \tag{A.7}$$
$$\dot{C}_{\tau\tau}^{T\,LL} = -2\,\alpha_e\, Q_l^2 \left(C_{\tau\tau}^{S\,LL} - 2 C_{\tau\tau}^{T\,LL} \right). \tag{A.8}$$

The running of the scalar and tensorial quark operators is given by

$$\dot{C}_{qq}^{S\,LL} = \left(-6\,\alpha_e \left(Q_l^2 + Q_q^2 \right) - 6 C_F\, \alpha_s \right) C_{qq}^{S\,LL} - 96\,\alpha_e\, Q_l Q_q C_{qq}^{T\,LL} + m_q k_{gg} C_{gg}^L, \tag{A.9}$$
$$\dot{C}_{qq}^{S\,LR} = \left(-6\,\alpha_e \left(Q_l^2 + Q_q^2 \right) - 6 C_F\, \alpha_s \right) C_{qq}^{S\,LR} + m_q k_{gg} C_{gg}^L, \tag{A.10}$$
$$\dot{C}_{qq}^{T\,LL} = -2\,\alpha_e\, Q_l Q_q C_{qq}^{S\,LL} + \left(2\,\alpha_e \left(Q_l^2 + Q_q^2 \right) + 2 C_F\, \alpha_s \right) C_{qq}^{T\,LL}, \tag{A.11}$$

where

$$k_{gg} = 96\pi\, C_F\, \alpha_s^2 m_\mu G_F. \tag{A.12}$$

Finally, the gluon operator is defined in eq. (2.8) such that its Wilson coefficient does not run at one loop, $\dot{C}_{gg}^L = \dot{C}_{gg}^R = 0$ [67].

Open Access. This article is distributed under the terms of the Creative Commons Attribution License (CC-BY 4.0), which permits any use, distribution and reproduction in any medium, provided the original author(s) and source are credited.

JHEP05(2017)117

References

[1] MEG collaboration, A.M. Baldini et al., *Search for the lepton flavour violating decay $\mu^+ \to e^+\gamma$ with the full dataset of the MEG experiment*, Eur. Phys. J. **C 76** (2016) 434 [arXiv:1605.05081] [INSPIRE].

[2] MEG collaboration, J. Adam et al., *New constraint on the existence of the $\mu^+ \to e^+\gamma$ decay*, Phys. Rev. Lett. **110** (2013) 201801 [arXiv:1303.0754] [INSPIRE].

[3] SINDRUM collaboration, U. Bellgardt et al., *Search for the Decay $\mu^+ \to e^+e^+e^-$*, Nucl. Phys. **B 299** (1988) 1 [INSPIRE].

[4] SINDRUM II collaboration, W.H. Bertl et al., *A Search for muon to electron conversion in muonic gold*, Eur. Phys. J. **C 47** (2006) 337 [INSPIRE].

[5] A.M. Baldini et al., *MEG Upgrade Proposal*, arXiv:1301.7225 [INSPIRE].

[6] A. Blondel et al., *Research Proposal for an Experiment to Search for the Decay $\mu \to eee$*, arXiv:1301.6113 [INSPIRE].

[7] DeeMe collaboration, M. Aoki, *An experimental search for muon-electron conversion in nuclear field at sensitivity of 10^{-14} with a pulsed proton beam*, AIP Conf. Proc. **1441** (2012) 599 [INSPIRE].

[8] Mu2e collaboration, R.M. Carey et al., *Proposal to search for $\mu^- N \to e^- N$ with a single event sensitivity below 10^{-16}*, FERMILAB-PROPOSAL-0973 [INSPIRE].

[9] R.K. Kutschke, *The Mu2e Experiment at Fermilab*, arXiv:1112.0242 [INSPIRE].

[10] COMET collaboration, Y.G. Cui et al., *Conceptual design report for experimental search for lepton flavor violating $\mu^- - e^-$ conversion at sensitivity of 10^{-16} with a slow-extracted bunched proton beam (COMET)*, KEK-2009-10 [INSPIRE].

[11] R.J. Barlow, *The PRISM/PRIME project*, Nucl. Phys. Proc. Suppl. **218** (2011) 44 [INSPIRE].

[12] M. Lindner, M. Platscher and F.S. Queiroz, *A Call for New Physics: The Muon Anomalous Magnetic Moment and Lepton Flavor Violation*, arXiv:1610.06587 [INSPIRE].

[13] Y. Kuno and Y. Okada, *Muon decay and physics beyond the standard model*, Rev. Mod. Phys. **73** (2001) 151 [hep-ph/9909265] [INSPIRE].

[14] S. Davidson, D.C. Bailey and B.A. Campbell, *Model independent constraints on leptoquarks from rare processes*, Z. Phys. **C 61** (1994) 613 [hep-ph/9309310] [INSPIRE].

[15] M. Carpentier and S. Davidson, *Constraints on two-lepton, two quark operators*, Eur. Phys. J. **C 70** (2010) 1071 [arXiv:1008.0280] [INSPIRE].

[16] B.M. Dassinger, T. Feldmann, T. Mannel and S. Turczyk, *Model-independent analysis of lepton flavour violating tau decays*, JHEP **10** (2007) 039 [arXiv:0707.0988] [INSPIRE].

[17] A. Celis, V. Cirigliano and E. Passemar, *Model-discriminating power of lepton flavor violating τ decays*, Phys. Rev. **D 89** (2014) 095014 [arXiv:1403.5781] [INSPIRE].

[18] A. Celis, V. Cirigliano and E. Passemar, *Disentangling new physics contributions in lepton flavour violating τ decays*, Nucl. Part. Phys. Proc. **273-275** (2016) 1664 [arXiv:1409.4439] [INSPIRE].

[19] M. Raidal et al., *Flavour physics of leptons and dipole moments*, Eur. Phys. J. **C 57** (2008) 13 [arXiv:0801.1826] [INSPIRE].

JHEP05(2017)117

[20] A.J. Buras, *Weak Hamiltonian, CP-violation and rare decays*, hep-ph/9806471 [INSPIRE].

[21] A. Czarnecki and E. Jankowski, *Electromagnetic suppression of the decay $\mu \to e\gamma$*, Phys. Rev. **D 65** (2002) 113004 [hep-ph/0106237] [INSPIRE].

[22] A. Czarnecki, W.J. Marciano and A. Vainshtein, *Refinements in electroweak contributions to the muon anomalous magnetic moment*, Phys. Rev. **D 67** (2003) 073006 [*Erratum ibid.* **D 73** (2006) 119901] [hep-ph/0212229] [INSPIRE].

[23] W. Buchmüller and D. Wyler, *Effective Lagrangian Analysis of New Interactions and Flavor Conservation*, Nucl. Phys. **B 268** (1986) 621 [INSPIRE].

[24] B. Grzadkowski, M. Iskrzynski, M. Misiak and J. Rosiek, *Dimension-Six Terms in the Standard Model Lagrangian*, JHEP **10** (2010) 085 [arXiv:1008.4884] [INSPIRE].

[25] E.E. Jenkins, A.V. Manohar and M. Trott, *Renormalization Group Evolution of the Standard Model Dimension Six Operators II: Yukawa Dependence*, JHEP **01** (2014) 035 [arXiv:1310.4838] [INSPIRE].

[26] R. Alonso, E.E. Jenkins, A.V. Manohar and M. Trott, *Renormalization Group Evolution of the Standard Model Dimension Six Operators III: Gauge Coupling Dependence and Phenomenology*, JHEP **04** (2014) 159 [arXiv:1312.2014] [INSPIRE].

[27] A. Crivellin, S. Najjari and J. Rosiek, *Lepton Flavor Violation in the Standard Model with general Dimension-Six Operators*, JHEP **04** (2014) 167 [arXiv:1312.0634] [INSPIRE].

[28] G.M. Pruna and A. Signer, *The $\mu \to e\gamma$ decay in a systematic effective field theory approach with dimension 6 operators*, JHEP **10** (2014) 014 [arXiv:1408.3565] [INSPIRE].

[29] R. Alonso, B. Grinstein and J. Martin Camalich, $\mathrm{SU}(2) \times \mathrm{U}(1)$ *gauge invariance and the shape of new physics in rare B decays*, Phys. Rev. Lett. **113** (2014) 241802 [arXiv:1407.7044] [INSPIRE].

[30] R. Alonso, B. Grinstein and J. Martin Camalich, *Lepton universality violation and lepton flavor conservation in B-meson decays*, JHEP **10** (2015) 184 [arXiv:1505.05164] [INSPIRE].

[31] L. Calibbi, A. Crivellin and T. Ota, *Effective Field Theory Approach to $b \to s\ell\ell^{(\prime)}$, $B \to K^{(*)}\nu\overline{\nu}$ and $B \to D^{(*)}\tau\nu$ with Third Generation Couplings*, Phys. Rev. Lett. **115** (2015) 181801 [arXiv:1506.02661] [INSPIRE].

[32] J. Aebischer, A. Crivellin, M. Fael and C. Greub, *Matching of gauge invariant dimension-six operators for $b \to s$ and $b \to c$ transitions*, JHEP **05** (2016) 037 [arXiv:1512.02830] [INSPIRE].

[33] S. Davidson, *$\mu \to e\gamma$ and matching at m_W*, Eur. Phys. J. **C 76** (2016) 370 [arXiv:1601.07166] [INSPIRE].

[34] S. Davidson, *$\mu \to e\gamma$ in the 2HDM: an exercise in EFT*, Eur. Phys. J. **C 76** (2016) 258 [arXiv:1601.01949] [INSPIRE].

[35] V. Cirigliano, R. Kitano, Y. Okada and P. Tuzon, *On the model discriminating power of $\mu \to e$ conversion in nuclei*, Phys. Rev. **D 80** (2009) 013002 [arXiv:0904.0957] [INSPIRE].

[36] T. Appelquist and J. Carazzone, *Infrared Singularities and Massive Fields*, Phys. Rev. **D 11** (1975) 2856 [INSPIRE].

[37] M.A. Shifman, A.I. Vainshtein and V.I. Zakharov, *Remarks on Higgs Boson Interactions with Nucleons*, Phys. Lett. **B 78** (1978) 443 [INSPIRE].

JHEP05(2017)117

[38] R. Kitano, M. Koike and Y. Okada, *Detailed calculation of lepton flavor violating muon electron conversion rate for various nuclei*, *Phys. Rev.* **D 66** (2002) 096002 [*Erratum ibid.* **D 76** (2007) 059902] [hep-ph/0203110] [INSPIRE].

[39] O.U. Shanker, *Z Dependence of Coherent μe Conversion Rate in Anomalous Neutrinoless Muon Capture*, *Phys. Rev.* **D 20** (1979) 1608 [INSPIRE].

[40] A. Czarnecki, W.J. Marciano and K. Melnikov, *Coherent muon electron conversion in muonic atoms*, *AIP Conf. Proc.* **435** (1998) 409 [hep-ph/9801218] [INSPIRE].

[41] SINDRUM II collaboration, C. Dohmen et al., *Test of lepton flavor conservation in $\mu \to e$ conversion on titanium*, *Phys. Lett.* **B 317** (1993) 631 [INSPIRE].

[42] SINDRUM II collaboration, W. Honecker et al., *Improved limit on the branching ratio of $\mu \to e$ conversion on lead*, *Phys. Rev. Lett.* **76** (1996) 200 [INSPIRE].

[43] A. Crivellin, M. Hoferichter and M. Procura, *Improved predictions for $\mu \to e$ conversion in nuclei and Higgs-induced lepton flavor violation*, *Phys. Rev.* **D 89** (2014) 093024 [arXiv:1404.7134] [INSPIRE].

[44] M. Hoferichter, J. Ruiz de Elvira, B. Kubis and U.-G. Meißner, *High-Precision Determination of the Pion-Nucleon σ Term from Roy-Steiner Equations*, *Phys. Rev. Lett.* **115** (2015) 092301 [arXiv:1506.04142] [INSPIRE].

[45] A. Crivellin, M. Hoferichter and M. Procura, *Accurate evaluation of hadronic uncertainties in spin-independent WIMP-nucleon scattering: Disentangling two- and three-flavor effects*, *Phys. Rev.* **D 89** (2014) 054021 [arXiv:1312.4951] [INSPIRE].

[46] P. Junnarkar and A. Walker-Loud, *Scalar strange content of the nucleon from lattice QCD*, *Phys. Rev.* **D 87** (2013) 114510 [arXiv:1301.1114] [INSPIRE].

[47] J.M. Alarcon, J. Martin Camalich and J.A. Oller, *The chiral representation of the πN scattering amplitude and the pion-nucleon sigma term*, *Phys. Rev.* **D 85** (2012) 051503 [arXiv:1110.3797] [INSPIRE].

[48] J.M. Alarcon, L.S. Geng, J. Martin Camalich and J.A. Oller, *The strangeness content of the nucleon from effective field theory and phenomenology*, *Phys. Lett.* **B 730** (2014) 342 [arXiv:1209.2870] [INSPIRE].

[49] T. Suzuki, D.F. Measday and J.P. Roalsvig, *Total Nuclear Capture Rates for Negative Muons*, *Phys. Rev.* **C 35** (1987) 2212 [INSPIRE].

[50] A.J. Buras, M. Jamin, M.E. Lautenbacher and P.H. Weisz, *Effective Hamiltonians for $\Delta S = 1$ and $\Delta B = 1$ nonleptonic decays beyond the leading logarithmic approximation*, *Nucl. Phys.* **B 370** (1992) 69 [INSPIRE].

[51] A. Alloul, N.D. Christensen, C. Degrande, C. Duhr and B. Fuks, *FeynRules 2.0 — A complete toolbox for tree-level phenomenology*, *Comput. Phys. Commun.* **185** (2014) 2250 [arXiv:1310.1921] [INSPIRE].

[52] T. Hahn, *Generating Feynman diagrams and amplitudes with FeynArts 3*, *Comput. Phys. Commun.* **140** (2001) 418 [hep-ph/0012260] [INSPIRE].

[53] T. Hahn and M. Pérez-Victoria, *Automatized one loop calculations in four-dimensions and D-dimensions*, *Comput. Phys. Commun.* **118** (1999) 153 [hep-ph/9807565] [INSPIRE].

[54] T. Hahn, S. Paßehr and C. Schappacher, *FormCalc 9 and Extensions*, PoS(LL2016)068 [arXiv:1604.04611] [INSPIRE].

JHEP05(2017)117

[55] J. Kuipers, T. Ueda, J.A.M. Vermaseren and J. Vollinga, *FORM version 4.0*, *Comput. Phys. Commun.* **184** (2013) 1453 [arXiv:1203.6543] [INSPIRE].

[56] M. Misiak, *On The dimensional methods in rare b decays*, *Phys. Lett.* **B 321** (1994) 113 [hep-ph/9309236] [INSPIRE].

[57] M. Ciuchini, E. Franco, L. Reina and L. Silvestrini, *Leading order QCD corrections to $b \to s\gamma$ and $b \to sg$ decays in three regularization schemes*, *Nucl. Phys.* **B 421** (1994) 41 [hep-ph/9311357] [INSPIRE].

[58] A. Crivellin, S. Davidson, G.M. Pruna and A. Signer, *Complementarity in lepton-flavour violating muon decay experiments*, arXiv:1611.03409 [INSPIRE].

[59] A. Crivellin, F. D'Eramo and M. Procura, *New Constraints on Dark Matter Effective Theories from Standard Model Loops*, *Phys. Rev. Lett.* **112** (2014) 191304 [arXiv:1402.1173] [INSPIRE].

[60] F. D'Eramo, B.J. Kavanagh and P. Panci, *You can hide but you have to run: direct detection with vector mediators*, *JHEP* **08** (2016) 111 [arXiv:1605.04917] [INSPIRE].

[61] A. Crivellin, G. D'Ambrosio, M. Hoferichter and L.C. Tunstall, *Violation of lepton flavor and lepton flavor universality in rare kaon decays*, *Phys. Rev.* **D 93** (2016) 074038 [arXiv:1601.00970] [INSPIRE].

[62] A. Crivellin, L. Hofer, J. Matias, U. Nierste, S. Pokorski and J. Rosiek, *Lepton-flavour violating B decays in generic Z' models*, *Phys. Rev.* **D 92** (2015) 054013 [arXiv:1504.07928] [INSPIRE].

[63] F. Feruglio, P. Paradisi and A. Pattori, *Revisiting Lepton Flavor Universality in B Decays*, *Phys. Rev. Lett.* **118** (2017) 011801 [arXiv:1606.00524] [INSPIRE].

[64] D. Black, T. Han, H.-J. He and M. Sher, *$\tau - \mu$ flavor violation as a probe of the scale of new physics*, *Phys. Rev.* **D 66** (2002) 053002 [hep-ph/0206056] [INSPIRE].

[65] F. Feruglio, *Theoretical Aspects of Flavour and CP-violation in the Lepton Sector*, arXiv:1509.08428 [INSPIRE].

[66] G.M. Pruna and A. Signer, *Lepton-flavour violating decays in theories with dimension 6 operators*, *EPJ Web Conf.* **118** (2016) 01031 [arXiv:1511.04421] [INSPIRE].

[67] V.P. Spiridonov, *Anomalous Dimension of $G^2_{\mu\nu}$ and β Function*, IYaI-P-0378 [INSPIRE].

JHEP05(2017)117